IDEA League

Master of Science in Applied Geophysics

Research Thesis

Estimating the lithium content in a hydrothermal reservoir using a modelling-based sensitivity analysis

Case study at the location Horstberg

Hauke H. Fehnker

August 5, 2022

Estimating the lithium content in a hydrothermal reservoir using a modelling-based sensitivity analysis

Case study at the location Horstberg

Master of Science Thesis

for the degree of Master of Science in Applied Geophysics

by

Hauke H. Fehnker

August 5, 2022

IDEA LEAGUE
JOINT MASTER'S IN APPLIED GEOPHYSICS

TU Delft, The Netherlands
ETH Zürich, Switzerland
RWTH Aachen, Germany

Dated: *August 5, 2022*

Supervisor(s):

Prof. Florian Wellmann

Dr. Katharina Alms

Committee Members:

Prof. Florian Wellmann

Dr. Cédric Schmelzbach

Eidesstattliche Versicherung

Fehnker, Hauke Heinrich | 420953

Name, Vorname | Matrikelnummer (freiwillige Angabe)

Ich versichere hiermit an Eides Statt, dass ich die vorliegende Arbeit/Bachelorarbeit/ Masterarbeit* mit dem Titel

Estimating the Lithium content in a hydrothermal reservoir using a modelling-based sensitivity analysis: Case study at the location Horstberg

selbständig und ohne unzulässige fremde Hilfe erbracht habe. Ich habe keine anderen als die angegebenen Quellen und Hilfsmittel benutzt. Für den Fall, dass die Arbeit zusätzlich auf einem Datenträger eingereicht wird, erkläre ich, dass die schriftliche und die elektronische Form vollständig übereinstimmen. Die Arbeit hat in gleicher oder ähnlicher Form noch keiner Prüfungsbehörde vorgelegen.

Aachen, 05.08.2022 | _____

Ort, Datum | Unterschrift

*Nichtzutreffendes bitte streichen

Belehrung:

§ 156 StGB: Falsche Versicherung an Eides Statt

Wer vor einer zur Abnahme einer Versicherung an Eides Statt zuständigen Behörde eine solche Versicherung falsch abgibt oder unter Berufung auf eine solche Versicherung falsch aussagt, wird mit Freiheitsstrafe bis zu drei Jahren oder mit Geldstrafe bestraft.

§ 161 StGB: Fahrlässiger Falscheid; fahrlässige falsche Versicherung an Eides Statt

(1) Wenn eine der in den §§ 154 bis 156 bezeichneten Handlungen aus Fahrlässigkeit begangen worden ist, so tritt Freiheitsstrafe bis zu einem Jahr oder Geldstrafe ein.

(2) Straflosigkeit tritt ein, wenn der Täter die falsche Angabe rechtzeitig berichtigt. Die Vorschriften des § 158 Abs. 2 und 3 gelten entsprechend.

Die vorstehende Belehrung habe ich zur Kenntnis genommen:

Aachen, 05.08.2022 | _____

Ort, Datum | Unterschrift

Abstract

The North German basin holds high potential for geothermal lithium exploration. Yet, so far, the assessment of reservoirs concentrates on locations in the Upper Rhine Graben. This thesis gives an example for the evaluation of a potential geothermal lithium reservoir of the Middle Buntsandstein at the location Horstberg in Lower Saxony. The targeted layers are part of the Solling and the Detfurth formation.

To determine the porosities and volumes of the two potential reservoir layers, including their uncertainties, well log data and a structural model are evaluated. The model is created using *Gempy*, an open-source library to create 3-D models in Python. Based on the estimated parameters and data from the literature, the lithium and heat quantities stored in place are estimated. Furthermore, calculations are carried out that target the design and production volume of a geothermal doublet with a theoretical production rate of 24 L/s.

For the Solling, the resulting mean quantities are 13,836 t of lithium and a stored heat of 2.59 - 3.04 $\mathrm{GJ\,m^{-2}}$. The values of the Detfurth are much lower. The amount of stored lithium amounts to 3,773 t and the heat-in-place is determined to be 1.85 - 2.19 $\mathrm{GJ\,m^{-2}}$. Regarding the calculations of the doublet, depending on the input parameters, the mean required distance between injection and production well is 1,037 - 2,021 m. Based on these results, 8-28 doublets would fit in the study area. One doublet system could produce 540.6 - 660.5 t of LCE per year.

Overall, the conditions for geothermal lithium exploration at Horstberg are rather poor. The reservoir is mainly limited by its low thickness and low production rate. Nevertheless, this study gave a good example of how to assess a potential geothermal lithium reservoir in the North German Basin.

Acknowledgements

First of all, I want to thank Prof. Florian Wellmann and Dr. Katharina Alms for supervising my thesis. Furthermore, I would like to thank Dr. Cédric Schmelzbach for examining this thesis together with Prof. Wellmann.

Special thanks go to Alexander Jüstel, who supported me mentally as well as with his expertise. I also want to thank him for proofreading my thesis. Moreover, I would like to thank Felix Jagert for his expertise with regard to well logging.

Also, I would like to thank the BGR for providing the data and the Fraunhofer IEG for making this project possible.

Finally, I want to thank all of my friends and my family, who supported me throughout this entire master's program.

RWTH Aachen University
August 5, 2022

Hauke H. Fehnker

Table of Contents

List of Figures

List of Tables

Acronyms

API American Petroleum Institute

BGR German Federal Institute for Geosciences and Natural Resources

EV Electric vehicle

HIP Heat-in-place

LCE lithium carbonate equivalent

URG Upper Rhine Graben

Chapter 1

Introduction

The following sections will address the relevance of sustainable lithium production and give an overview of prior projects targeting geothermal lithium exploration in Germany. Furthermore, the research approach of this thesis will briefly be described.

1-1 Importance of sustainable lithium exploration

Throughout the past decades, the importance of lithium has risen enormously. This is mainly due to its use in lithium-ion batteries, which are required for electric vehicles (EV). Over the past decade, the global amount of battery-driven EVs has already risen from 0.02 million in 2010 to 4.79 million in 2019. For future development, the International Energy Agency (IEA) has examined two different scenarios. The "Stated Policies Scenario" takes into account all so far decided government policies and predicts an increase of EVs to a total amount of 140 million by 2030. This amount would correspond to 7 % of all global vehicles. The "Sustainable Development Scenario" predicts a development following the climate goals of the Paris Agreement. Thus, the growth would be even bigger and mount to a total number of 245 million EVs by 2030 [IEA, 2020].

When it comes to production and usage of lithium, the global shares are very unequally distributed. While 90 % of all EV sales are made in China, Europe and the US, the production of lithium is concentrated in Australia, Chile, China and Argentina (fig 1-1). Thus, especially Europe and the US are heavily dependent on the resources of foreign countries, when facing the challenge of developing and producing more sustainable vehicles to counteract the consequences of climate change.

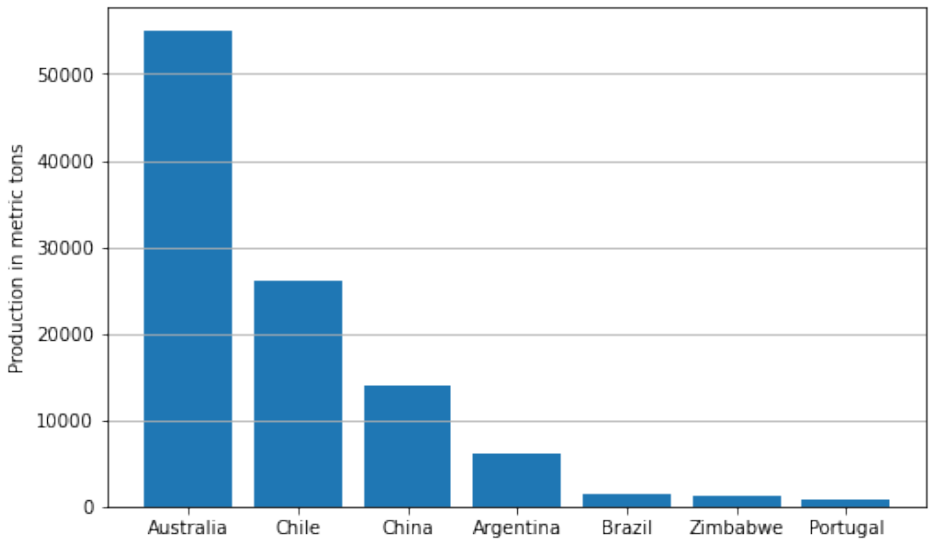

Figure 1-1: Lithium production of the biggest producing countries. Values from U.S. Geological Survey, 2022.

Comparing the two countries with the biggest lithium production, Australia and Chile, the two main types of lithium repositories can be comprehended. In Australia, the main source of lithium is hard-rock pegmatite repositories. The pegmatite is extracted using conventional mining methods, which makes it relatively energy consuming and expensive. On the other hand, the lithium concentration in pegmatites is relatively high, which accounts for those costs. Although the lithium resources of Australia include only 7.3 million tons, which is much less than the reserves of South American countries, its production value of 55,000 tons in 2021 is by far the highest in the world. This amount corresponds to more than half of the global production volume [U.S. Geological Survey, 2022].

In Chile and many other locations in South America, lithium is contained in brines, which are found in salars, the most famous one being the Salar de Atacama with a total surface area of about 3000 km^2. Chile's lithium reserves are the largest in the world and are estimated to be 9.8 million tons in total. Yet, its production value of 26,000 t is still less than half of the production in Australia [U.S. Geological Survey, 2022]. The extraction of the lithium from the brine occurs through evaporation. Calcium sulfate, salt and other components of the brine are separated, which leads to an increase in the lithium concentration. This process is very water-consuming, which causes socio-environmental conflicts. Especially with regards to the indigenous communities in Chile, it is criticized that the water resources of the global South are exploited for the production of resources, which are used mainly for EVs in the global North [Jerez et al., 2021].

Due to these developments, attempts are made to make the production of lithium more sustainable. This includes recycling wasted lithium batteries, but also the developing of methods to extract lithium more sustainably from natural resources. One example is the extraction from geothermal reservoirs, which is considered below. In theory, this method could lead to lithium production with low water consumption and zero CO_2 emissions [Bundesverband Geothermie, 2021].

1-2 Lithium from geothermal reservoirs

As the demand for lithium increases and current production in foreign countries is not very sustainable, many European countries, including Germany, have started searching for alternative local lithium repositories. Especially extracting lithium from geothermal brines has proven to be very promising [Warren, 2021]. The idea is to extract both simultaneously, lithium and geothermal energy. Accordingly, this method requires a repository with two major characteristics, high lithium concentration (>150 mg/L) and a high geothermal gradient. In Europe, only six geothermal areas have been found that contain fluids with such high lithium concentrations. Three of these areas, the North German Basin, the Upper Rhine Graben and the Molasse Basin are located in Germany [Sanjuan et al., 2022].

In the past years, particularly the Upper Rhine Graben drew attention to itself. It is part of the European Cenozoic Rift System and is mainly located along the German-French border between Frankfurt in the North and Basel (Switzerland) in the South. The local lithium concentration in the geothermal fluids amounts to 120 - 220 mg/L. According to the first estimations, a reservoir area of 15×15 km contains 200,000 - 300,000 t of lithium. One single geothermal doublet could produce up to 2,000 t of lithium carbonate per year [Bundesverband Geothermie, 2021]. Although this production value and also the reserves are much less than in the main producing countries Australia and Chile, such more sustainable exploration holds the chance to make Germany and Europe less dependent on foreign countries, e.g. regarding the production of EVs [Tabelin et al., 2021].

To expand European lithium production, it is important to exploit further sources. Besides the Upper Rhine Graben, also the North German Basin contains promising areas with high lithium concentrations and geothermal gradients [Sanjuan et al., 2022]. Those locations still need to be examined more closely to finally assess if geothermal lithium exploration is possible and can be profitable. In this thesis, the location Horstberg will be used to give an example of how such an assessment can be carried out.

1-3 The location Horstberg

Horstberg is located in the German state of Lower Saxony, 15 km southwest of Uelzen. The location is named after a hill, which at the location of interest has an elevation of 105 m above sea level. In 1987, the German oil and gas company BEB started natural gas exploration at the location Horstberg. For this purpose, the gas well *Horstberg Z1* with a total depth of 4,395 m was drilled, which in 2003 has been taken over by the German Federal Institute for Geosciences and Natural Resources (BGR) [W Rühaak et al., 2018]. From 2003 until 2018 it was utilized for the *GeneSys* project to investigate the exploration of geothermal energy. In this project, two sandstone layers in the Solling and the Detfurth formation were connected, by creating an artificial crack through hydraulic stimulation. The idea behind this procedure was to let the water circulate through only one single well, as shown in figure 1-2 [Tischner, 2018].

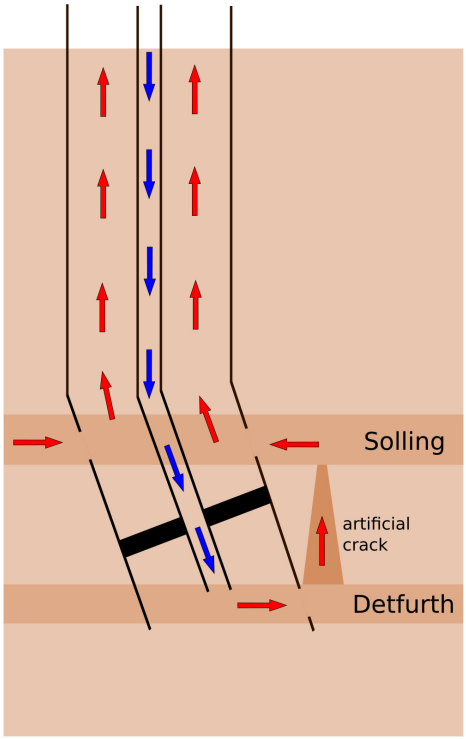

Figure 1-2: Visualization of the circulation through one well, performed at Horstberg during the GeneSys project. Based on Tischner, 2018.

Although the artificial crack could be created successfully, the flow rate of the circulation could not be kept at a satisfying level [BGR, 2008]. The more usual approach to generate geothermal energy is a doublet system, where two wells are utilized, one each for injection and production [Stober and Bucher, 2013]. While the circulation through one single well utilized at Horstberg is relatively new, geothermal doublets have already been investigated more comprehensively since the 1970s, e.g. targeting their life span [Gringarten, 1978]. Such doublet systems are also used for lithium extraction from geothermal reservoirs in the Upper Rhine Graben [Sanjuan et al., 2022]. Due to these circumstances, this thesis will focus on the potential lithium extraction from a doublet and not from a single well.

To evaluate the potential lithium exploration, first of all, it will be investigated if the amount of stored lithium in the reservoir is sufficient for exploration. For the geothermal lithium exploration, the potential to generate geothermal energy from the reservoir also plays a big role. Due to that, in addition to the stored lithium quantity, also the amount of stored heat will be calculated. The potential reservoir layers would be the same sandstone layers as investigated during the *GeneSys* project. Many different parameters must be considered, e.g. the porosity of the host rock, the thickness of the reservoir layer and the lithium concentration in the formation fluid. For the potential doublet system, it will be crucial to determine the required distance between injection and production wells and to estimate how much of the stored lithium can be extracted from the reservoir. Finally, all results must be evaluated with respect to their uncertainties. Furthermore, they will be compared to the values from the Upper Rhine Graben.

1-4 Overview of research approach

To derive the required parameters which are missing to assess the lithium and heat content in the reservoir, many different steps are executed. First of all, a general overview of the geology will help to characterize the reservoir. Next, the recreation of an existing subsurface model in the area of the Horstberg Z1 well will provide information about the geometry of the reservoir layers and the influences of the fault system.

Another important part is the evaluation of log data from the *Horstberg Z1* well. Here, it must be taken into account that the results are based on 1-D data. Thus, for physical parameters and further information derived from it, large uncertainty will be assumed. Information derived from the log data will include estimates for porosity, layer thickness and clay content.

The results obtained from the research of the *GeneSys* project will also be very helpful to investigate if the geothermal exploration of lithium is possible at the location Horstberg. They include information about the geology and physical properties of the Buntsandstein formation, as well as measured lithium concentrations of the deep geothermal fluids.

Once all parameters are derived, the lithium content and the heat stored in the study area will be assessed using volumetric calculations. Furthermore, based on an analytic solution for the design of a geothermal doublet, it will be investigated how much lithium could be extracted from the reservoir over a certain period. The resulting values will be compared to those found in the Upper Rhine Graben. The overall workflow can be comprehended in figure 1-3.

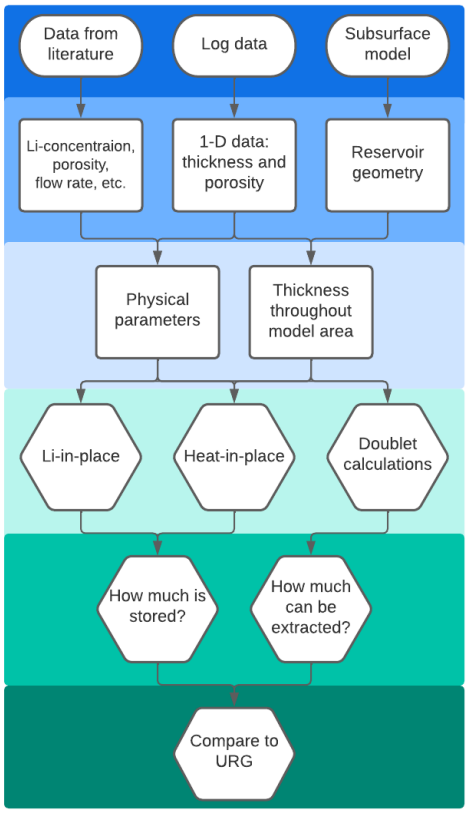

Figure 1-3: Visualization of the workflow of this Master thesis.

Chapter 2

Geology

The location Horstberg lies in the North German Basin, which, belonging to the Southern Permian Basin, is part of the Central European Basin System. It extends from the Southern North Sea to the Western Baltic Sea and mainly includes the Northern parts of the Netherlands as well as the North German Mainland [Brink, 2005]. The deposited sediments inside the basin are characterized by layers of siliciclastic rocks, carbonates and salt, which originate from both, continental and maritime deposition [Bundesverband Geothermie, 2020]. Also, the potential reservoir layers are part of these deposited sediments. They belong to the Solling and the Detfurth formation, which are stratigraphic sections of the Middle Buntsandstein.

In most parts of the North German Basin, the Buntsandstein is superimposed by Mesozoic and Cenozoic sediments. Thus, most information about the Middle Buntsandstein facies originates from boreholes [Röhling, 2014]. This is also the case for the location Horstberg. Overall, sandstones from the Buntsandstein in North Germany tend to have an advanced maturity, meaning that due to long ways of material transport less resistant minerals are filtered out and the grains are well-rounded [Franz et al., 2015]. This is can be explained by the fact that the material of the sandstones originated from areas in the south, like the Bohemian Massif [Röhling, 2014].

In general, the North German Basin is characterized by the presence of many tectonic structures. In the area of interest, this shows through two faults, which cause a major displacement in the Buntsandstein formation. Their orientation is very similar, both dipping in the NNW-SSE direction. They are both located almost parallel at the eastern border of the study area and are running out towards the center, forming a ramp-like structure. There are also other faults in the area, but these will be neglected, as they do not affect the Buntsandstein formation [Steuer, 2016].

Other important geological structures in the North German Basin are salt domes. Although in the study area none of them are present, their presence could be of relevance, if the research area is expanded laterally. Overall, six major salt structures on the level of the Middle Buntsandstein can be found near the study area (fig 2-1) [Baldschuhn et al., 2001].

Both targeted layers store Mesozoic deep fluids. For the North German Basin, it is assumed that Mesozoic fluids originate from pore water which is trapped during the sedi-

mentation. Most of them are very salty as they originally were brackish water or seawater [Stober et al., 2014]. The fluids are especially of interest for this study as they store the Lithium and could be extracted to generate geothermal energy. The exploration of geothermal energy at Horstberg has already been investigated in detail during the GeneSys project [BGR, 2008].

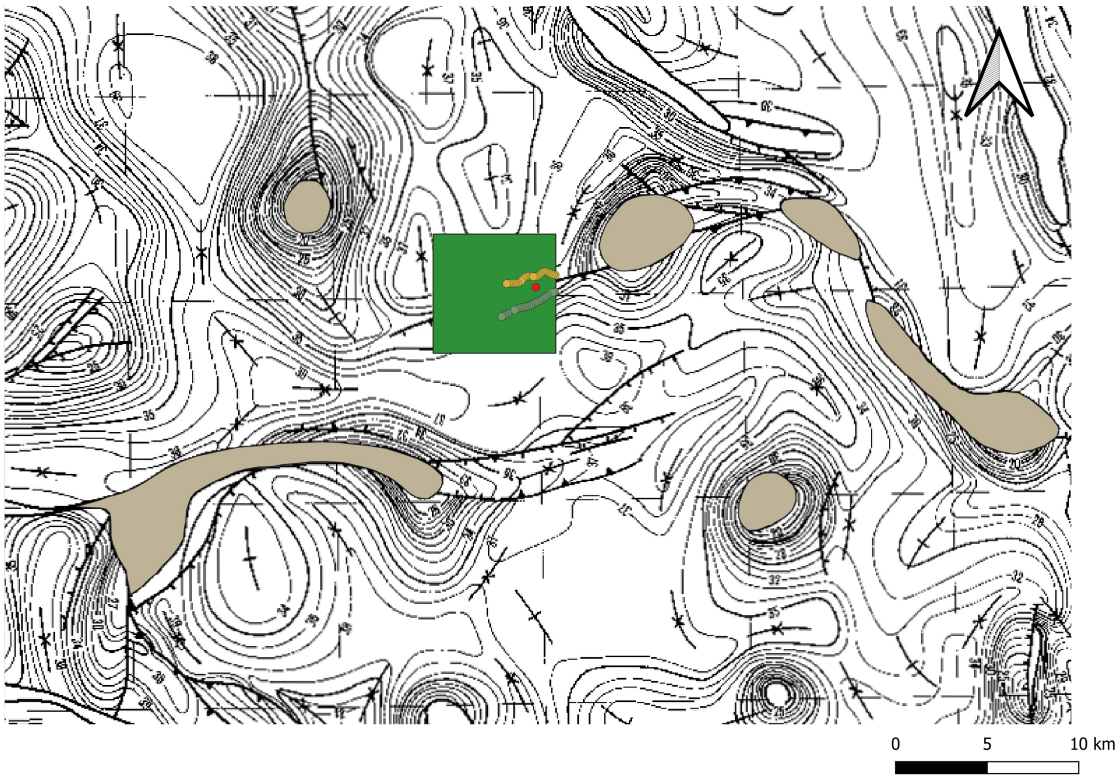

Figure 2-1: Strucutral map of the Middle Buntsandstein [Baldschuhn et al., 2001]; The green rectangle marks the investigation area, including the Horstberg Z1 well (red dot) and the position of the two major faults (green and yellow dots). The brownish areas are the salt structures close to the investigation area.

Chapter 3

Materials and Methods

This chapter first describes what information can be derived from the results of the *GeneSys* project, which targeted the exploration of geothermal energy at the location Horstberg. Secondly, it will be described how and based on what kind of data the investigations targeting the stored lithium and heat will be performed.

3-1 Review of the GeneSys project

The *GeneSys* project at the location Horstberg was conducted by the BGR from 2003 to 2018 and aimed to investigate the geothermal exploration using only one well for both, production and injection (fig 1-2) [BGR, 2008]. The layers of the Solling and Detfurth, which were the objectives of the *GeneSys* project will also be the target of the investigation of potential lithium exploration. Thus, many results of the project are helpful for the investigation of this master thesis. These results will be presented in the following section.

A report by Tischner et al. (2015) contains information about physical parameters of the rocks and a geochemical analysis of the stored fluids. To determine the porosity of each layer, resistivity measurements were carried out, which showed a porosity of 11 % for the Solling sandstone and 8-8.5 % for the Detfurth sandstone [Gerling et al., 2015]. Using another method based on acoustic log measurements, the porosities will be further investigated in this research project and compared to those from the *GeneSys* project.

Another parameter that is relevant for the potential exploration of lithium is the production rate. The maximum flow rate for the circulation through one well was 25 l/s. Although the created artificial crack was of high permeability, this rate could not be maintained for longer time periods. Overall, it was evaluated that the Solling sandstone has a higher productivity than the Detfurth. Yet, it was concluded that the production rate is too low for a classical doublet system [Gerling et al., 2015]. However, the extraction of lithium through a geothermal doublet might be an attractive method for for other locations. As this thesis should give an example on how to assess the potential for geothermal lithium exploration, it will

be evaluated, how much quantity could be extracted from a doublet system if the conditions were better. This topic will be addressed further in section 3-7.

Also the lithium concentration of the formation fluid has been analysed based on samples which were taken from the well. For the fluid in the Solling formation a concentration of 202 mg/l was measured, while the Detfurth had a value of 92 mg/l. Two other measurements, where the sample was a mix of the fluids from both formations resulted in 201 mg/l and 123 mg/l [Gerling et al., 2015]. The report also included information about the temperatures of the reservoir. The temperature of the fluid that could potentially be extracted from the reservoir was estimated to be 140°C [Gerling et al., 2015].

The thicknesses of the Solling and Detfurth layers are described in different publications, yet the published results are not always consistent. Regarding the Solling sandstone, the thickness at the locaiton of the well is given as 18 m by Rühaak et al. (2018). Yet, in a report of Steuer (2016) a geological profile is presented, which indicates that the Solling sandstone has a thickness of ~ 20 m. Part of this thesis will be to evaluate the log data from the location Horstberg to eliminate this discrepancy. The thickness of the other potential reservoir layer of the Detfurth sandstone was determined to be 14 m. This result will also be discussed by analysing the log data.

Generally, from the results of the *GeneSys* project, it can already be concluded that, in terms of volumetric storage, the Solling sandstone is the more promising reservoir for geothermal lithium exploration, as it has a higher thickness, porosity and lithium concentration in its formation fluid. Although the content in the Detfurth layer is lower, it could still represent a potential reservoir. Therefore, both horizons are considered in this work.

3-2 Available data

The data to determine the parameters required for the assessment of the lithium and heat storage consists of two parts. Both parts originate from the prior investigations at Horstberg reviewed in section 3-1 and were provided by the BGR.

The first part is log data from the former gas well *Horstberg Z1*, more precisely gamma ray and acoustic data, as well as the corresponding geological profile, which is based on the rocks encountered during the drilling (fig 3-1). For this kind of data it is of high importance, to take into account that it is one dimensional. Thus, it only gives information about the parameters at one specific location, which might not be representative for the entire reservoir. Yet, for many parameters the logging results will be the best clues, as no further data is available.

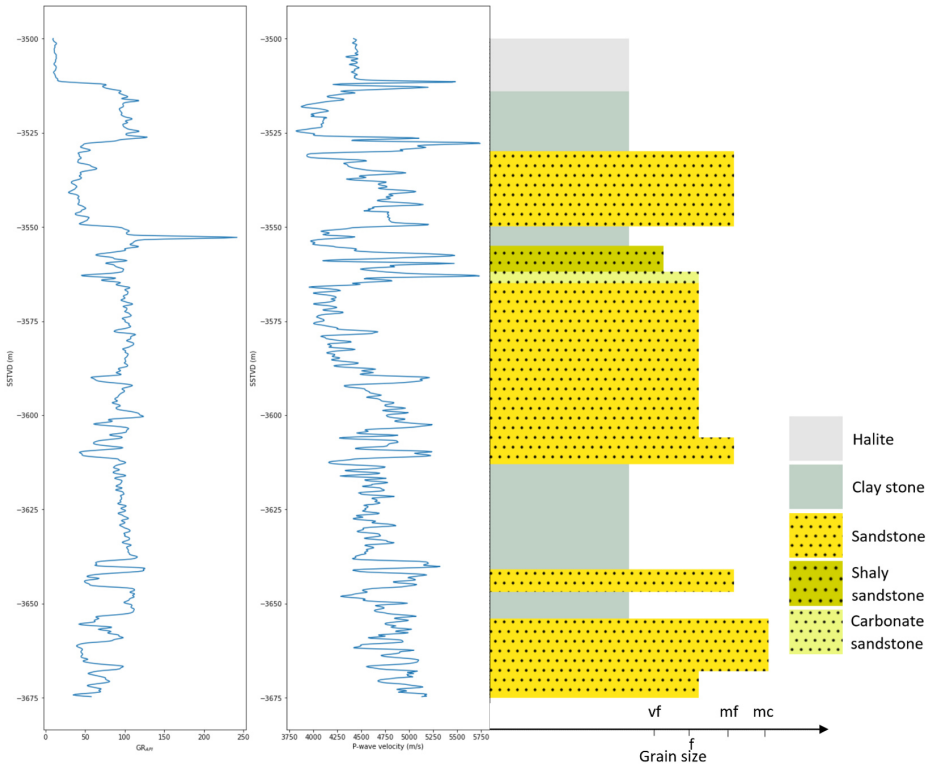

Figure 3-1: From left to right: provided gamma ray data, provided acoustic log data and geological profile (based on Steuer (2016)).

The second part of the data is a 3-D structural model of the subsurface around the *Horstberg Z1* well. It is based on measurements from a 3-D seismic cube, where the reflections were assigned to the geological horizons, based on the borehole profile of the well. The provided model consists of interface points representing the base of each interpreted stratigraphic horizon and the faults. The modelled area has a size of 6,700 × 6,500 m. In vertical direction, the targeted part of the Middle Buntsandstein covers a depth range of 3466 - 3939 m.

In this project the focus lies on the Solling and the Detfurth formation. The Hadegsen formation shows a thickness which is too low to be represented in the model and will be seen as part of the Detfurth formation in this case. In total, the Solling base consits of 67,161 points and the Detfurth of 67,069. As an upper boundary of the model, the base of the Upper Buntsandstein is used, which consists of 66,998 points. The two major faults which are present in the model area are represented by 708 and 789 points.

For purposes of reproducibility, the model is recreated in GemPy (https://www.gempy.org/), which is an open-source tool to generate geological models in Python. To reduce the required computational time and power only a share of all provided interface points is used to create the model in GemPy.

3-3 Logging

Logging is a powerful tool, which allows geophysicists to gain 1-D information about the subsurface at a specific location and depth. Therefore, a measurement device, which is attached to a wire is lowered down the borehole at constant speed. Thereby, it usually performs continuous measurements [Ellis and Singer, 2007]. In this case, the types of measurements performed were gamma ray and acoustic logging. The measured data was sampled every 15 cm.

3-3-1 Gamma ray

For the investigation of geothermal lithium exploration, the gamma ray logging serves two purposes. First of all, the thicknesses of the reservoir layers is investigated, which will be crucial to analyse how much lithium is stored in the target formation. Secondly, shale contents of different layers can be investigated. High clay content leads to a low permeability of a rock. Thus, using the gamma ray data it will particularly be studied how the permeability of the reservoir can be assessed compared to its surrounding cap- and bedrock.

The principle of gamma ray logging is to measure gamma rays resulting from natural radioactive decay. Those natural radioactive sources include the decay of ^{40}K, ^{232}Th and ^{238}U. Each of these isotopes can be characterized through a specific spectrum of emitted gamma ray energy during the decay. Mainly Potassium, but also Thorium and Uranium are highly represented in minerals that are typically found in sedimentary rocks. Especially clay minerals often have high Potassium concentrations and can therefore be well detected using gamma ray logging devices. The measurement is scaled in American Petroleum Institute (API) units, which is a calibration standard based on an artificial radioactive formation. It is designed to fit a radioactivity, which is twice as high as that of typical shale and is given by the following formula:

$$GR_{API} = \alpha^{238}U_{ppm} + \beta^{232}Th_{ppm} + \gamma^{39}K_{\%}, \tag{3-1}$$

where α, β and γ correspond to factors chosen depending on the measurement device used and the subscripts correspond to the unit of mass concentration used for each of the isotopes [Ellis and Singer, 2007].

A rock type containing high amounts of clay minerals is shale. Log analysts even use the two terms shale and clay interchangeably. Under the assumption that a gamma ray measurement contains results from both, a formation containing no shale at all and a formation consisting of pure shale or respectively clay (100 %), it is possible to calculate the shale content of every other unit using the so called gamma ray index:

$$I_{GR} = \frac{\gamma_{log} - \gamma_{min}}{\gamma_{max} - \gamma_{min}}, \tag{3-2}$$

where γ_{log} is the measured GR_{API} value for an arbitrary formation, γ_{min} is the measured GR_{API} value for 0 % shale and γ_{max} is the measured GR_{API} value for 100 % shale.

The relation between I_{GR} and shale volume is not always linear. Depending on the rock type, there are different recommendations on how the correlation should be implemented [Ellis and Singer, 2007]. In 1969, Larionov proposed the following imperic formula for Mesozoic rocks, like those of the Middle Buntsandstein [Szabó et al., 2014]:

$$V_{Sh} = 0.33 * (2^{2I_{GR}} - 1). \tag{3-3}$$

This correlation can be comprehended in figure 3-2. One big error source for this technique is that the formation with minimum GR_{API} value could still contain a low percentage of shale. This error source is minimized in the case of Horstberg, as the GR_{API} value, which is chosen to be 0 % shale, results from a formation consisting of Halite, which usually only contains minor contents of Potassium and no Thorium or Uranium [Bonewitz, 2012].

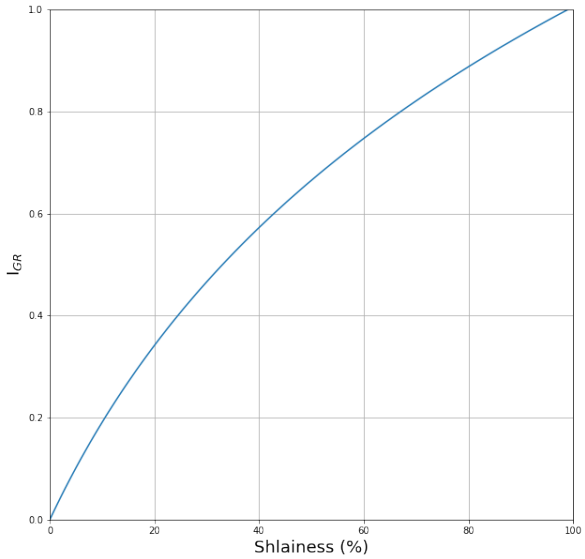

Figure 3-2: Relationship between I_{GR} and shaliness for Mesozoic rocks; Based on Szabó et al. (2014).

To check the Gamma ray data in terms of plausibility, the resulting shale contents for each depth is compared to the geological profile. It will then be examined if the layers in the profile correspond to characteristic shale contents and if their vertical extent matches the layer thicknesses in the profile. This particularely be of relevance to investigate the thickness of the Solling and the Detfurth reservoir layers.

3-3-2 Acoustic logging

The acoustic log data will be used to investigate the porosity of the two reservoir layers. This will be of high importance to study the total pore volume of the reservoir, which stores the lithium-containing fluid.

The conventional approach of acoustic logging is the transmission method, where a receiver measures the arrival of acoustic energy send out by a receiver located at some distance from

it. Thereby, the emitted acoustic wave travels through a part of the rock surrounding the borehole. The velocity and thus the arrival time of the propagating wave is material-depended. Typical velocities of compressional waves for salt, sandstone and shale can be comprehended in table 3-1. Based on the borehole profile and the values from table 3-1, the acoustic log data can be checked in terms of plausibility. For example the found Halite formation should correspond to values close to 15,000 ft/s (4,572 m/s) [Ellis and Singer, 2007].

Material	v_p (ft/s)	v_p (m/s)
Salt	15,000	4,572
Sandstone	11,500 - 16,500	3,505 - 5,029
Shale	7,000 - 17,000	2,134 - 5,182

Table 3-1: Table with typical velocities of compressional waves for salt, sandstone and shale. [Ellis and Singer, 2007]

In 1959 Wyllie et al. published experimental results, which show a linear correlation of porosity and interval transit time for saturated sandstones under conditions of high directional pressure (fig 3-3) [Ellis and Singer, 2007]. Using this correlation, for each sampled data point inside the reservoir layers, the porosity is determined. Its mean and standard deviation will lead to a range of plausible porosity values for each of the layers.

The results should be considered with caution, as the circumstances in the field probably differ from those in the laboratory (e.g. in terms of pressure and lithology of the sandstone). Yet, it still gives a good indication for what the porosity of the investigated sandstone layers might be. The porosities derived through acoustic logging will be compared to those, obtained using resistivity measurements during the *GeneSys* project.

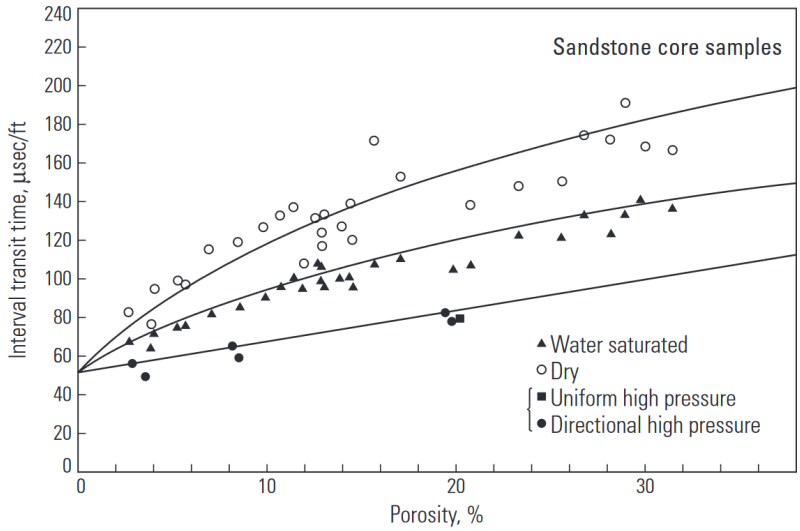

Figure 3-3: Relationship between v_p and porosity. The linear trend for directional high pressure is relevant for the investigations of this thesis. [Ellis and Singer, 2007]

3-4 Structural model

In this chapter, the re-creation of a structural model of the Middle Buntsandstein is targeted. Furthermore, it will be explained how based on this model the thicknesses of the reservoir layers are estimated.

3-4-1 Modelling in Gempy

The modelling is based on provided interface points, which represent the base of each stratigraphic horizon, as well as the two major faults that affect the Middle Buntsandstein at Horstberg. For each layer, these interface points are interpolated to form those horizons and faults. At the positions, where the horizons cross the faults, the presence of the faults must cause an offset. The model will provide information about this offset and the geometry and thickness of the reservoir layers. Such a structural model can be created in Gempy, which is an open-source python library, which can be used to construct 3D-geological models [GemPy.org, 2022].

Although for each stratigraphic horizon over 60,000 data points and for the faults over 700 points are available, not all of them will be used for the modelling, to increase computational efficiency and save data storage. Instead, the interface points are sampled in such a way that they evenly cover the model area. In total, three horizons had to be modelled: The base of the Upper Buntsandstein, defining the upper boundary of the model, the base of the Solling formation and the base of the Detfurth formation. Although the Hadegsen formation is located in-between the Solling and the Detfurth formation, it will not be modelled explicitly as its thickness is too low. Instead, the Hadegsen will be included in the Detfurth formation.

Besides importing the points, the associated orientations of the horizons and the faults need to be assigned, meaning information on how they are aligned in the geometric space. The horizons are assumed to be almost horizontal. Thus, a dip and azimuth of 0° are chosen. For the faults, an azimuth of 160° and a dip of 60° are defined, such that they dip in SSE-direction. These values are based on the data which was provided by the BGR.

Once the data is imported and the orientations are assigned, the size and resolution of the model must be defined. In this case, the model covers a rectangular area of size 6,700 × 6,500 m. The vertical expansion is chosen to be 600 m, which is slightly bigger than the total vertical extent of the investigated layers. This is done, to ensure that no information is cut off. The resolution is set to $100 \times 100 \times 100$, resulting in a total number of 1,000,000 voxels. This is the recommended maximum resolution. Adding much more does not improve the model significantly in terms of resolution, but increases the required computational time and power enormously.

The modelling process is based on a cokriging interpolation that considers the given interface points and the orientations. This kind of interpolation was first introduced by Lajaunie et al. (1997). To assure that the model distinguishes between stratigraphic layers and faults, classes are assigned to each group of interface points and orientations. At first, each fault and horizon is modeled individually before adding them all together. This procedure is carried out for the sake of clarity. The final result is visualized in an interactive 3-D plot. Throughout the modelling process, shares of interface points and orientations will be added or deleted,

until the final result appears to be geologically plausible. The Python code, which is used to create the model can be comprehended in the appendix.

3-4-2 Determination of the reservoir thickness

The provided structural model holds information about the thickness of the entrie Solling and Detfurth formations, but not of the potential reservoirs, which are just layers within these formations. Yet, they can be estimated under the assumption that the thicknesses of the reservoir layers behave similarly to those of the entire formations.

First of all, the thickness of the formations must be derived from the interfaces of the model. Therefore, three arrays were created, one each containing the points of the base of the Upper Buntsandstein, the Solling and the Detfurth. The idea is to subtract the depth coordinates of the Solling base from the Upper Buntsandstein base to obtain the thickness of the Solling formation and to subtract those of the Detfurth base from the Solling base to obtain the thickness of the Detfurth formation. Assuming that the layers are horizontal, the points to subtract must have the same X and Y coordinates. Thus, all points are filtered out that do not have corresponding points with the same X and Y coordinates in the array of the base below or above respectively. The depth difference of these points will be plotted as a contour plot in python using the python library Matplotlib. Such a map that visualizes the thickness variations of an area, is also referred to as *isopach map* [Tearpock and Bischke, 2002].

As the provided structural model did not contain any further information about the thickness of the reservoir layers, the only information available is the thickness estimated from the logging. Based on this value, the thicknesses of the reservoir layer are estimated for the entire model area. This is done by dividing the thickness throughout the entire formation through its thickness at the position of the well. This leads to a factor, which shows how much the thickness of the formation at each location of the model area deviates from the thickness at the position of the well (fig 4-16). Multiplying this factor with the estimated thickness of the reservoir layer at the well location results in the thickness of the reservoir layer throughout the model area, if the reservoir thickness behaved equally to that of the entire Solling formation. This perfect correlation is very unlikely, yet it is assumed that the mean thickness of the reservoir layer lies within the range of the standard deviation from the mean of the result for perfect correlation.

The described procedure is performed for both, the Solling and the Detfurth layer. The determined thicknesses will be essential for all further calculations.

3-5 Lithium-in-place analysis

Lithium-in-place analysis means to estimate the lithium content stored in a specific reservoir of limited lateral size. It is based on a volumetric calculation, which is comparable to the estimation of oil-in-place, which uses information on the reservoir properties (e.g. reservoir rocks and limits) to determine how much oil quantity is stored inside of it [Schanz Jr, 1979]. It is important to keep in mind that such an analysis does not give insight into how much of the stored quantity can be recovered. Yet, it can be used to estimate if the stored amount is worth further investigation or exploration and to rate and compare different sites.

For the calculation, it is assumed that all pores of the reservoir host rock are fully saturated. Based on this assumption, it is carried out based on the following formula:

$$m_{Li} = V_{res} \cdot \Phi \cdot c_{Li}, \tag{3-4}$$

where V_{res} is the volume of the reservoir layer, Φ is the porosity and c_{Li} is the lithium concentration of the formation fluid. In this case, the reservoir is laterally constrained by the boundaries of the model. Using the results from the logging and the model of the subsurface, the thickness of the reservoir layer throughout the model area will be estimated. These calculations are carried out for both, the Solling and the Detfurth layer. The porosity will be estimated using the results of the logging and the measured values from the resistivity measurements, which were part of the *GeneSys* project. Regarding the lithium concentrations of the stored fluid, the only source will be the measured values from the *GeneSys* project.

All of those parameters have certain inaccuracies. These are taken into account by the use of error propagation, such that in the end a range of possible end results is calculated. The error propagation is based on the following formula:

$$\Delta m_{Li} = \sqrt{\left(\Delta V_{res} \cdot \frac{\delta m_{Li}}{\delta V_{res}}\right)^2 + \left(\Delta \phi \cdot \frac{\delta m_{Li}}{\delta \Phi}\right)^2 + \left(\Delta c_{Li} \cdot \frac{\delta m_{Li}}{\delta c_{Li}}\right)^2} \tag{3-5}$$

To make the result comparable to other locations, especially the Upper Rhine Graben, the stored lithium amount per reservoir area will be calculated:

$$m_{Li,norm} = \frac{m_{Li}}{A_{res}} \tag{3-6}$$

The input parameters for formulas 3-4 - 3-6 are based on previous results and literature data from the *GeneSys* project. The volume V_{res} is derived by multiplying the model area A_{res} with the mean layer thickness h, which is determined using the model and the results from the gamma ray logging. The porosity Φ will be taken from the acoustic logging and the lithium concentration c_{Li} is based on the literature of the *GeneSys* project (204 mg/L; [Gerling et al., 2015]).

Due to the area being constant, ΔV_{res} is only dependent on the error of the thickness Δh. For Δh and $\Delta \Phi$, the standard deviations from the logging results will be used. For the lithium concentration of the fluid, only one measured value from the *GeneSys* project is available for each potential reservoir layer. Also, no further information about the measurements is available, which makes it difficult to assess the accuracy of the values. Yet, a general measurement error of 10 % is assumed. Based on the error propagation, minimum and maximum values for the stored amount of lithium m_{Li} are estimated.

3-6 Heat-in-place analysis

Heat-in-place is a method to assess the quantity of heat or respectively thermal energy, which is stored in a geothermal reservoir. The temperature used to estimate the stored heat is always taken with respect to a reference value, which is often the re-injection temperature. Thus, it refers to the amount of heat that can be theoretically extracted from the reservoir [Muffler and Cataldi, 1978]. The formula to calculate the quantity of heat stored per reservoir area is given as follows:

$$H = h \cdot (T_{prod} - T_{inj}) \cdot \gamma, \tag{3-7}$$

where h is the aquifer thickness and T_{prod} and T_{inj} are the temperatures of the fluid extracted from the production well and the re-injection temperature. γ is the bulk heat capacity parameter which is defined as:

$$\gamma = \Phi \cdot c_w \cdot \rho_w + (1 - \Phi) \cdot c_r \cdot \rho_r, \tag{3-8}$$

where Φ denotes the aquifer porosity, c_w and c_r represent the heat capacity of the fluid and the aquifer rock and $_w$ and $_r$ are their corresponding densities [Muffler and Cataldi, 1978].

Similarly to the lithium-in-place analysis, again many parameters have a range of uncertainty, which is again accounted for by the use of error propagation. Furthermore, the result of the heat-in-place analysis must be reviewed with caution, as it only represents an estimation of the potential but not the actual amount of heat or energy that can be recovered from the reservoir. This is because the recovery factor is not taken into account. This factor represents the share of the available resource that can actually be recovered from the reservoir. Regarding this, for geothermal energy, it must also be considered that during the exploration additional heat could be supplied to the reservoir by external sources.

For h and Φ, the same values are assumed as for the lithium-in-place analysis, which are based on the results from the logging. All other input parameters will be taken from literature and can be comprehended in table 3-2.

Input parameter	Value
T_{prod} (°C)	140*
T_{inj} (°C)	60**
ρ_w (g cm^{-3})	1***
ρ_r (g cm^{-3})	2***
c_w (kJ kg^{-1} K^{-1})	4.12**
c_r (kJ kg^{-1} K^{-1})	0.82 - 1.0**

Table 3-2: Input parameters to calculate the heat-in-place.
*[Gerling et al., 2015]
**[Stober and Bucher, 2013]
***[Schön, 2016]

3-7 Doublet calculations

In section 3-1 it was already described that prior investigations came to the result that due to the low permeabilities of the reservoir layers at the location of the well, and low production rates resulting from that, the installation of a geothermal doublet would be impossible [Gerling et al., 2015]. Yet, in this thesis, it will be investigated how a doublet should be designed and how much lithium could be extracted from the reservoir, if the production rate was higher. This is done to evaluate if a reservoir with conditions similar to that at Horstberg could keep up with those of other locations, like the Upper Rhine Graben. For this theoretical calculation, only the Solling layer will be considered as it has the larger thickness, porosity and lithium concentration.

A doublet is the most popular system to extract heat from a geothermal reservoir. It consists of a production and an injection well. Through the production well the thermal fluid will be extracted from the reservoir. At the surface, the thermal energy is transferred to a heat exchanger. Thereby, the extracted fluid is cooled down and afterwards is re-injected into the reservoir (fig 3-4). This procedure is carried out to remain constant pressure in the reservoir and thus prevent subsidence events. Or in other words: the water that has been extracted must be replaced. The re-injection also serves the purpose of waste management. The cooled water still contains gases and dissolved solids, which would be more expensive to be disposed differently [Stober and Bucher, 2013].

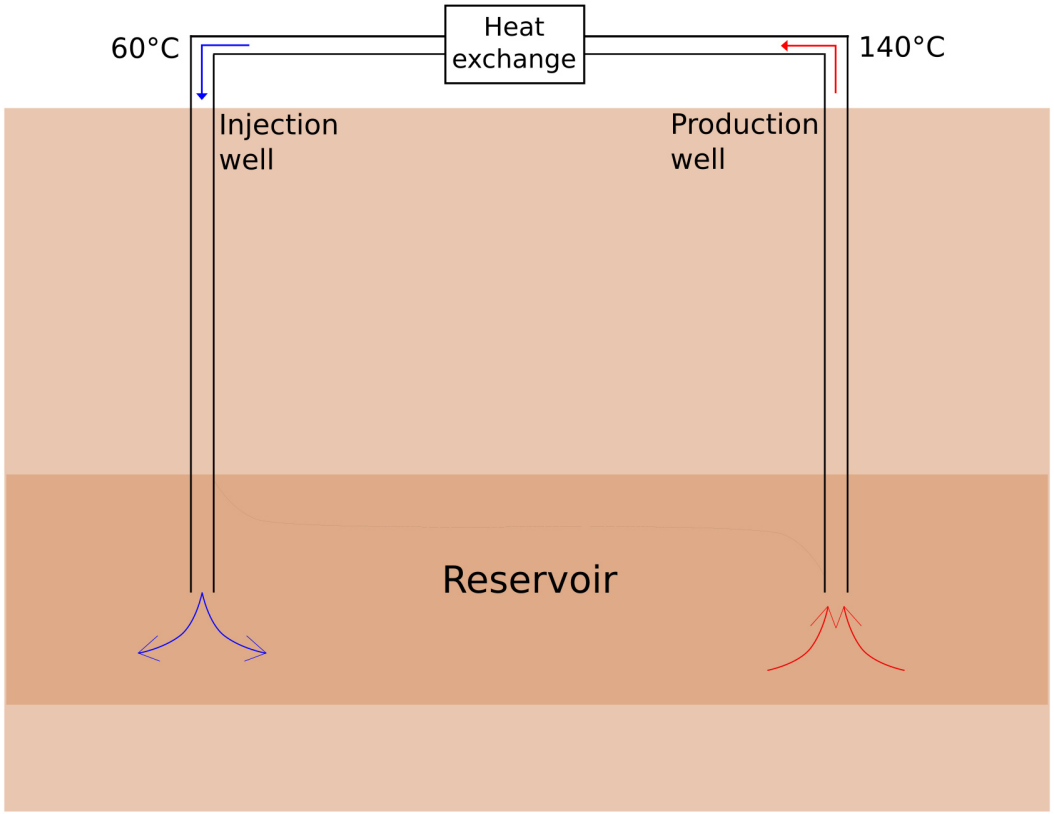

Figure 3-4: Main features of a geothermal doublet system.

Due to the re-injection, zones of cool water develop around the injection well, which increase over time and at some point reach the production well. Such a thermal breakthrough would result in an enormous reduction of efficiency of the doublet, as the water temperature at the production well would decrease [Gringarten and Sauty, 1975]. For lithium exploration, it would also have negative consequences, as the injected water is depleted in lithium.

To keep the injection and production well at the minimum distance which is required to avoid a thermal breakthrough caused by the injection of the cool water, an analytic solution has been presented by Gringarten and Sauty in 1975. This solution is derived for a horizontal aquifer of uniform thickness h with a constant injection rate Q, which is equal to the production rate. Furthermore, initial temperature differences between the aquifer, its cap rock and the bedrock are neglected. The formula to determine the optimal distance between injection and production well goes as follows:

$$D = \sqrt{\frac{2 \cdot Q \cdot \Delta t}{(\Phi + (1-\Phi)\frac{\rho_R c_R}{\rho_w c_w})h + \sqrt{(\Phi + (1-\Phi)\frac{\rho_R c_R}{\rho_w c_w})^2 h^2 + 2\frac{K_R \rho_R c_R}{(\rho_w c_w)^2}\Delta t}}}, \tag{3-9}$$

where Δt is the period of time that the doublet should run, Φ is the aquifer porosity, c_R and c_w are the heat capacity of the cap rock and the fluid and ρ_R and ρ_w are the densities of the cap rock and the fluid respectively. K_R is the thermal conductivity of the cap rock [Gringarten and Sauty, 1975]. Thus, longer time periods and higher injection rates require larger distances, as they contribute to the increase of the zones of cool water surrounding the injection well, while a high thickness leads to a smaller required distance. The effect of the porosity depends on the ratio $\frac{\rho_R c_R}{\rho_w c_w}$. If it is larger than 1, a high porosity leads to a higher required distance and vice versa. Furthermore, the closer $\frac{\rho_R c_R}{\rho_w c_w}$ is to 1, the less the porosity contributes to the end result.

The calculation will be performed for a varying thickness of the reservoir layer throughout the area. For the porosity, a range of possible values will be taken into account, based on the mean and standard deviation resulting from the acoustic log data. Due to the fact that the porosity is estimated based on one location only, it is assumed that the porosity does not vary throughout the whole area. Furthermore, the information about the physical parameters of the cap rock is deficient. From the borehole record, it is known that the cap rock is a clay stone. According to literature, clay stones have a range of possible densities, heat capacities and thermal conductivities. As no further information on the properties of the clay stone is available, those values are varied within these ranges. Furthermore, a safety factor of 5% will be added to the end result, to ensure that the distance between injection and production well is sufficient. As the aquifer thickness varies throughout the reservoir, different distances will be calculated for different parts of the reservoir.

The injection rate Q was chosen based on a range of sample values for the production rate in the North German Basin and a comparable Buntsandstein reservoir in the Upper Rhine Graben. In the North German Basin current production rates range from 11 - 35 L/s [Agemar et al., 2014]. Buntsandstein reservoirs of the URG show similar porosities compared to the Solling sandstone at Horstberg. A prominent example of a Middle Buntsandstein reservoir is the location Bruchsal. There, the production rate amounts to 24 L/s, which perfectly lies within the range of those from the North German Basin [Agemar et al., 2014]. This value

will also be assumed for this theoretical calculation at Horstberg. All input variables, besides the porosity Φ and the thickness h, are shown in table 3-3. Φ and h will be determined using the log data and the structural model.

Input parameter	Value
Q (L/s)	24*
Δ t (a)	30
ρ_w (g cm^{-3})	1**
ρ_r (g cm^{-3})	1.3 - 2.3**
c_w (kJ kg^{-1} K^{-1})	4.12***
c_r (kJ kg^{-1} K^{-1})	0.82 - 1.18**
K_r (W m^{-1} K^{-1})	0.6 - 4.0***

Table 3-3: Values of the input parameters to calculate the distance between injection and production well; Based on Gringarten and Sauty (1975).
*[Agemar et al., 2014]
**[Schön, 2016]
***[Stober and Bucher, 2013]

Once the calculations targeting the well distances are complete, the total amount of utilizable lithium from the reservoir is estimated using a method similar to the one used by Jung et al. (2002). To estimate the utilizable geothermal energy from the Molasse basin, they fictively covered the area with a grid of doublets and summed up the recoverable power for each of them [Jung et al., 2002]. Using the average of the determined required distances for injection and production well, the same will be done for the model area. Due to lack of information, no further area will be considered, although the reservoir could extend further than the model boundaries.

Using the production rate Q and recovery factor for the lithium, it can be calculated how much quantity can be extracted from one doublet. The annual production time is assumed to be 8,000 hours, as this matches the value assumed for the URG. The same applies to the recovery factor of the lithium, which is assumed to be 80 % [UnLimited, 2022]. The amount of the recovered lithium will be transformed into lithium carbonate equivalent (LCE), as lithium carbonate (Li_2CO_3) is the most common material from which lithium is extracted. The conversion factor to convert lithium to lithium carbonate is 5.323 [Bundesverband Geothermie, 2021]. The calculation to obtain the annual LCE production of one doublet goes as follows:

$$LCE_{annual} = Q \cdot t \cdot c_{Li} \cdot f_r \cdot f_c, \tag{3-10}$$

where Q is the production rate, t is the annual production time, c_{Li} is the lithium concentration (204 L/s), f_r is the recovery factor and f_c is the conversion factor. The potential annual production for the whole area is obtained by multiplying LCE_{annual} with the number of potential doublets.

3-8 Sensitivity analysis

In a sensitivity analysis, it is investigated which uncertain parameters of a numerical model have the largest influence on the end result. Thus, it is estimated how the final output varies with varying each sensitive variable. In mathematical terms, for a function $u = f(x)$ with the input $x = x_1, ..., x_n$, it is aimed to investigate the sensitivity of the required solution u* with respect to an input parameter x_k [Sobol, 2001]. Sensitivity analysis is used in a wide range of fields in research as well as in the free economy. Usual applications are in areas of decision making or assessing the riskiness of a strategy [Werbos, 1982].

In the case of this research, the sensitivity analysis will be rather simple, as most formulas used to derive the results show linear relationships between the parameters and the outcome. The two main sensitive parameters are the porosity and thickness of the reservoir. It will be investigated which of these parameters has the largest impact on the lithium-in-place analysis, Heat-in-place analysis. For the doublet calculations in addition to the thickness and porosity, also the impact of the cap rock parameters will be considered. Thereby, the cap rock parameters are summarized as the factor $K_r \rho_r C_r$. Just like in section 3-7, the sensitivity analysis will also only be performed for the Solling layer.

The relationship between the input parameters and the amount of Lithium which is stored in the reservoir is linear. Thus, the parameter with the largest relative uncertainty contributes the most to the uncertainty of the end result.

For the heat stored in place, the thickness h contributes linearly, while the porosity Φ is contained in the factor γ. Although this relationship is also linear, the contribution of Φ to the end result depends on the densities ρ_w and ρ_r and heat capacities c_w and c_r of the fluid and the aquifer rock. Due to $\frac{\rho_R c_R}{\rho_w c_w}$ being close to 1 for all considered cases, the porosity does not have a big impact on the end result. To quantify this impact, results were calculated while only varying h and Φ within their range of uncertainty and keeping all other values constant. It is then compared whether h or Φ caused the larger spread in the outcome.

Regarding the calculation of the required distance between the injection and production well, a similar procedure as for the heat-in-place is carried out. For different combinations of Φ, h and $K_r \rho_r C_r$ within their range of uncertainty, it is investigated which parameter causes the largest uncertainty of the end result.

The results of this study can be used to assess whether the accuracy of the end results and the parameters is sufficient or whether they would require further investigation to increase their reliability.

Chapter 4

Results

In this chapter, first, the results of the well logging and the structural modelling are described. Based on their outcome, the stored quantities of heat and lithium are estimated and the calculations targeting geothermal doublets are carried out.

4-1 Logging

In the following part, the results for the determined shale content, based on the calculated gamma ray index and the estimated porosities from the acoustic logging will be presented.

4-1-1 Gamma ray

First of all, the measured GR_{API} is plotted against the "Subsea True Vertical Depth" (SSTVD) (fig 4-1). The SSTVD range, which is considered will be from 3,500 m to 3,675 m, such that it covers the layers of the Solling and the Detfurth. Based on the minimum and maximum GR_{API} values, the gamma ray index I_{GR} is calculated for each data point 3-2. Finally, using formula 3-3, the shale volume is calculated based on the gamma ray index 4-2.

The highest shale value is calculated for a layer that according to the geological profile is clay stone. The lowest one is determined for the halite of the Upper Buntsandstein. The potential reservoir layer of the Solling formation shows a characteristic shale volume of 7.7 %. This characteristic volume has a vertical extent of 20.5 m from 3,529 - 3,549.5 m SSTVD. The layers lying above and below the potential reservoir show higher shale volumes. Most of them are in the range of 20-30 %.

Generally, at the depth of the potential reservoir of the Dethfurt formation, similar shale volumes are found as for the Solling layer. Yet, there is a section of higher volumes, which amount to up to 23 %. Due to this, the mean shale volume of the Detfurth layer is 12.9 %. The layer above shows a significantly higher volume of 28 %. The volume of the layer below is only slightly higher. Its mean is 13.6 %.

Based on the Gamma ray data, the thicknesses of the potential reservoirs are determined to be 20.5 m for the Solling sandstone and 13.7 m for the Detfurth sandstone.

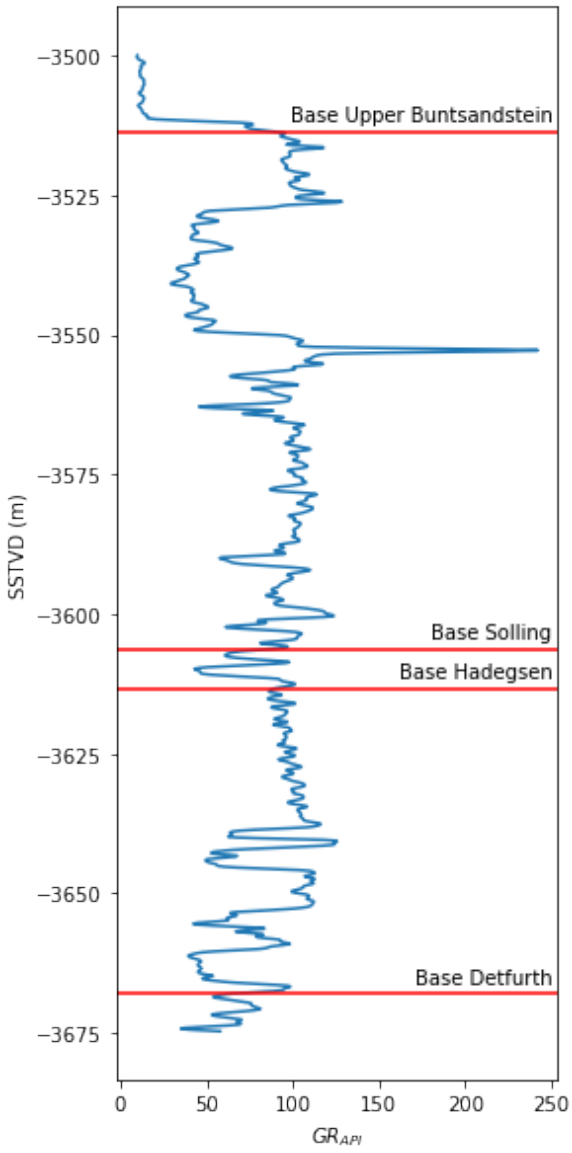

Figure 4-1: GR_{API} plotted in relation to depth (SSTVD). The red lines denote the positions of the stratigraphic boundaries (from top to bottom): Upper Buntsandstein base, Solling base, Hadegsen base, Detfurth base.

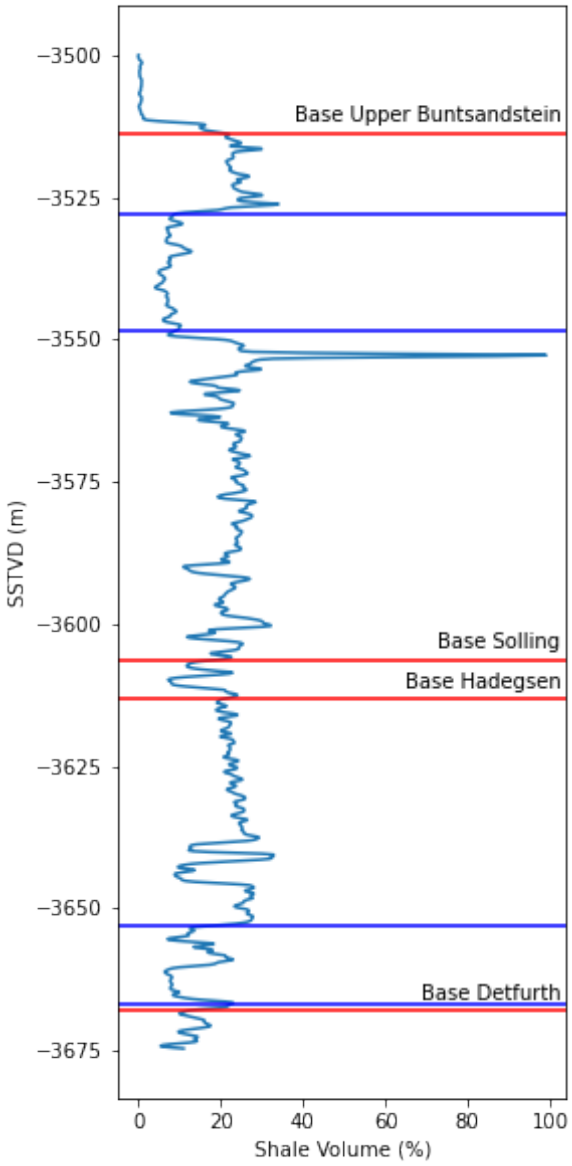

Figure 4-2: Shale volume plotted in relation to depth (SSTVD). The red lines denote the positions of the stratigraphic boundaries (from top to bottom): Upper Buntsandstein base, Solling base, Hadegsen base, Detfurth base. The blue lines denote the positions of the potential reservoir boundaries.

4-1-2 Acoustic logging

Also the acoustic data is plotted against the SSTVD (fig4-3). The investigated depth range of 3,500 m to 3,675 m is the same as for the gamma ray logging. Again, the part at the very top of the plot corresponds to the Halite formation from the Upper Buntsandstein. The measured mean velocity of this formation is 4,434 m/s.

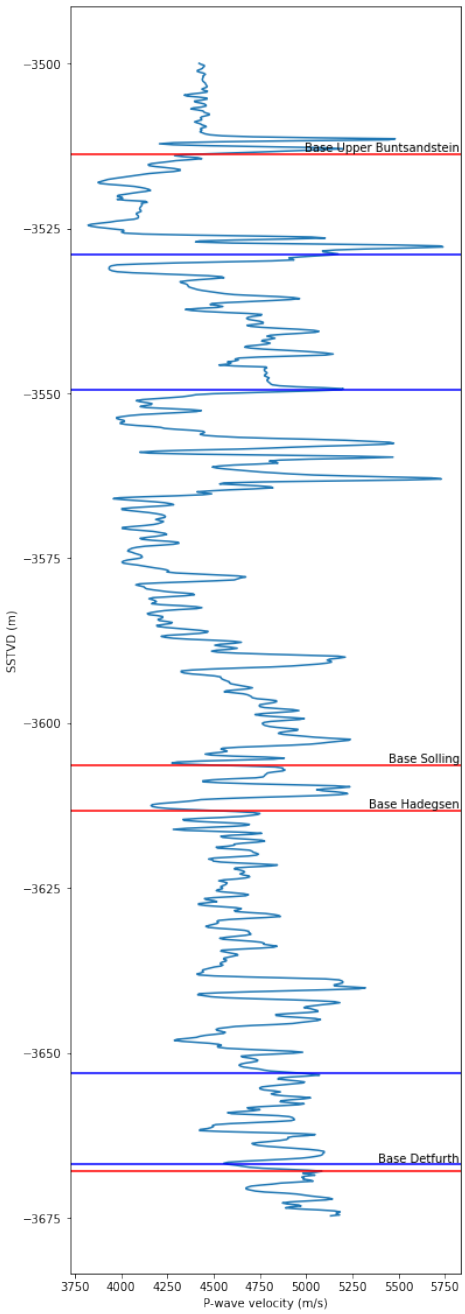

Figure 4-3: P-wave velocity plotted in relation to depth (SSTVD). The red lines denote the positions of the stratigraphic boundaries (from top to bottom): Upper Buntsandstein base, Solling base, Hadegsen base, Detfurth base. The blue lines denote the positions of the potential reservoir boundaries.

Using the linear correlation between acoustic velocity and porosity for saturated sandstones under high directional pressure conditions (fig 3-3), the measured velocities of the sandstone layers are converted into porosities (fig 4-4). The results are then plotted as histograms to evaluate which porosity appears in which frequency for each sandstone layer (fig 4-5). The amount of bins is thereby chosen via Sturges' rule, which decides on the bin number based

on sample size [Scott, 2009].

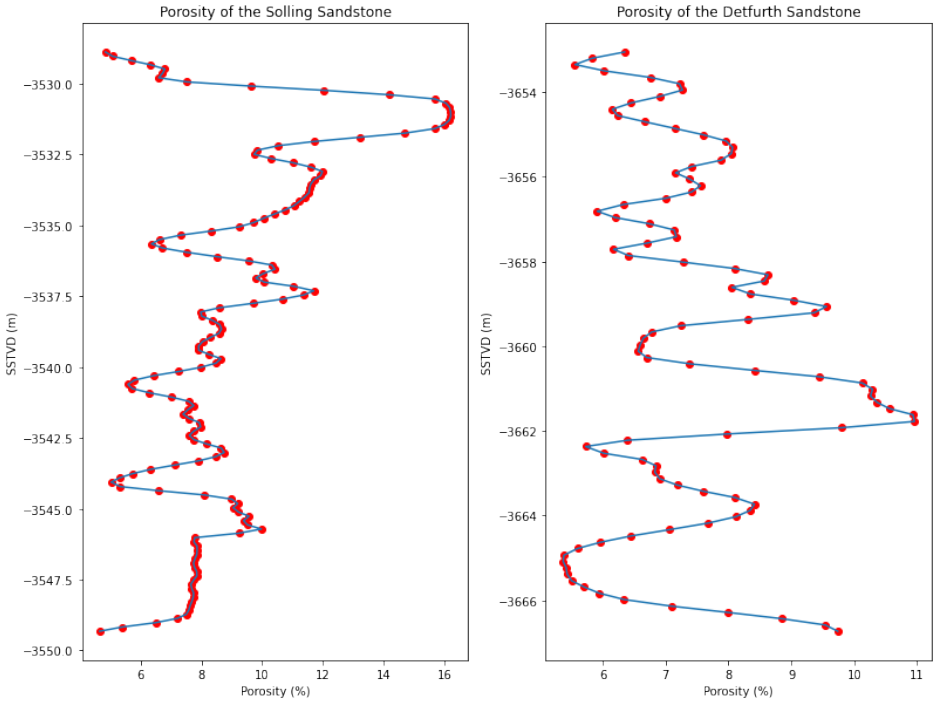

Figure 4-4: Porosities of the Solling and Detfurth sandstone calculated based on the acoustic log data. The red dots denote the data points sampled every 15 cm. The blue line is interpolated.

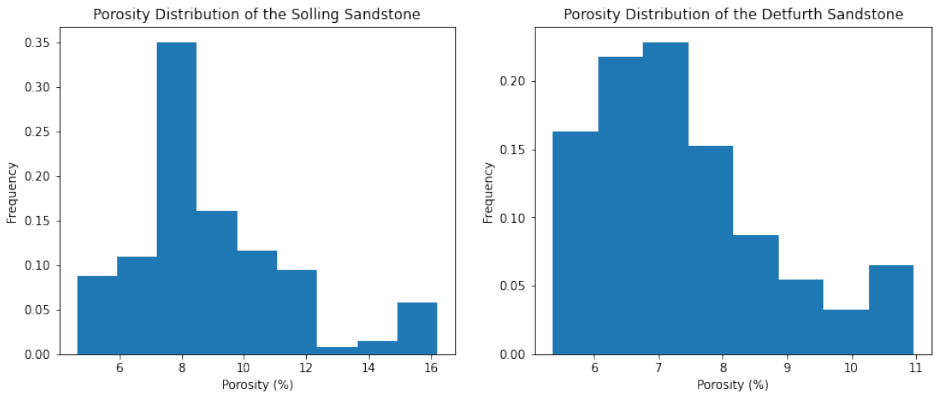

Figure 4-5: Histograms representing the frequency of different porosities for the Solling and Detfurth sandstone layer.

The most important result that can be evaluated from the histograms is that the Solling sandstone has a noticeably higher porosity than the Detfurth sandstone. For the Solling sandstone, the mean porosity is 8.96 % with a standard deviation of 2.59 %. The mean of the Detfurth amounts to 7.55 % with a standard deviation of 1.39 %. Thus, the mean values both lie beneath the porosity obtained from the resistivity measurements (11 % for Solling

and 8.5 % for Detfurth), yet those still lie within the range of the standard deviations.

For the Solling sandstone, the calculated porosities range from 4.64 % to 16.21 %. Taking a closer look at the plotted porosity in dependence of the SSTVD, a trend is recognizable, where the porosity decreases with depth. The Detfurth layer shows no such trend and the distribution appears to be arbitrary. The porosities range from 5.37 % to 10.96 %. Thus the values are less spread, compared to those of the Solling sandstone, which is also indicated by the lower standard deviation.

4-2 Strucutral model

In this section, the results of the modelling in Gempy, as well as the calculated thicknesses of the reservoir layers are described.

4-2-1 Modelling in Gempy

After importing the data and setting up the Gempy code in a Jupyter Notebook, the first part of the subsurface to be modelled were the two faults. Modelling their position and nature with sufficient accuracy is crucial as their orientation and dip must indicate the correct position of the fault offset. Another important aspect of the fault is that it is pinching out, meaning that it causes a large offset at the eastern edge of the model, which gets less towards the center and at some point fully disappears. This characteristic proved to be the most complicated part of the model and was targeted for each layer individually. Figure 4-6 shows the result for the base of the Detfurth formation.

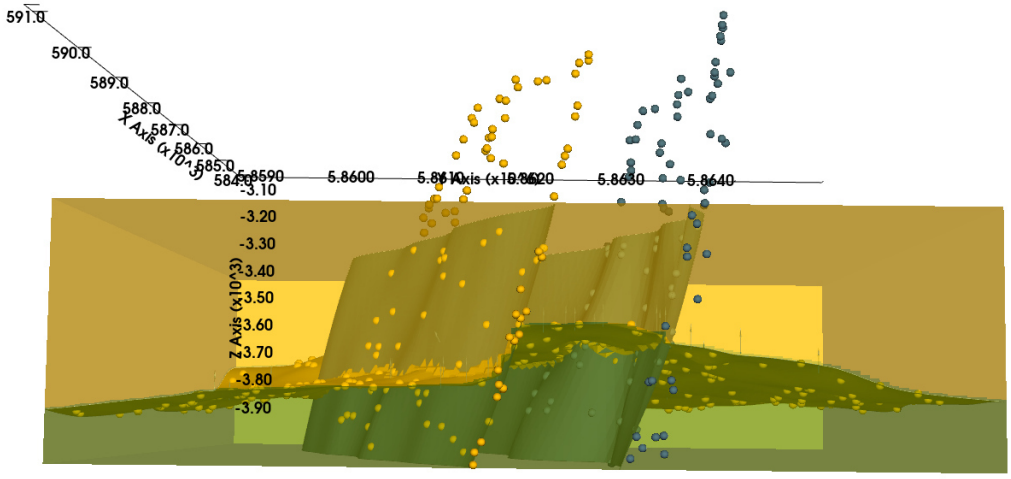

Figure 4-6: Intermediate result after modelling the base of the Detfurth layer, such that the faults show a clear offset that is pinching out.

To model each layer with high exactness, different shares of the interface points were used to represent the base of each horizon. The final chosen points are a mixture of evenly distributed

points throughout the entire area and a random choice of points surrounding the faults. Furthermore, some points were added individually at positions where geological characteristics have to be modelled more precisely (e.g. surrounding the faults). For the final result, approximately 180 points were used for the base of each horizon and 100 points for each of the two faults (fig 4-7).

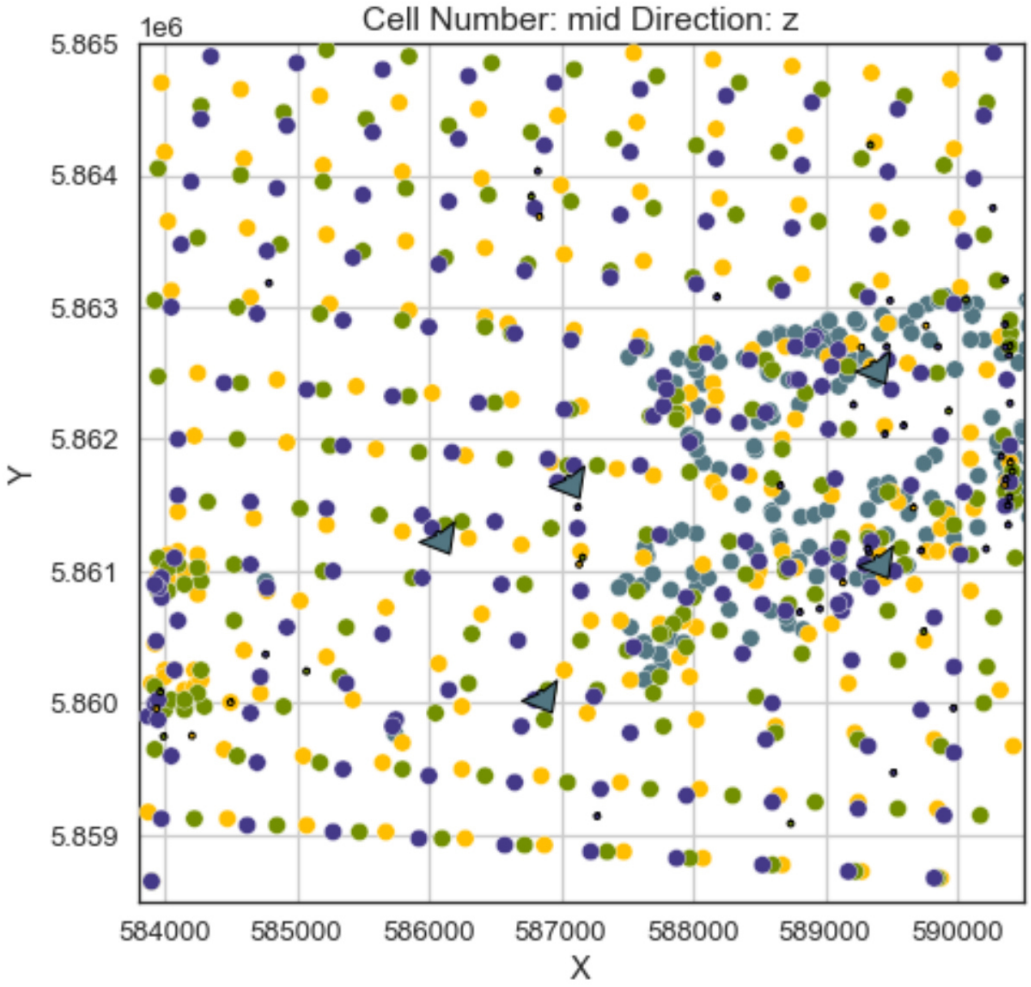

Figure 4-7: Overview of all interface points throughout the area, which were used to create the model. Yellow points: Base of the Upper Buntsandstein; Green points: Base of the Solling formation; Blue points: Base of the Detfurth formation; Grey points: Faults; Grey triangles: Orientations of the faults; Black dots: Orientations of the layers.

Each layer was adjusted until the final model, especially regarding the fault offset showed satisfying results (fig 4-8). As mentioned before, the outgoing characteristic was the biggest challenge. The biggest problem regarding this issue was that the fault would not stop causing an offset in the centre of the modelling area. Also in the final result, some artifacts of this issue are still present, yet they could be reduced to be minimal (fig 4-9).

The final model can be comprehended in figures 4-8 - 4-11. The orientation of the layers is predominantly horizontal. Deviations from this feature can only be found in the southwestern

part of the model, where the layers undergo a slight elevation and in-between the two faults, where the layers have a ramp-like structure. Overall, the thicknesses in the southern area of the model are bigger than in the northern part.

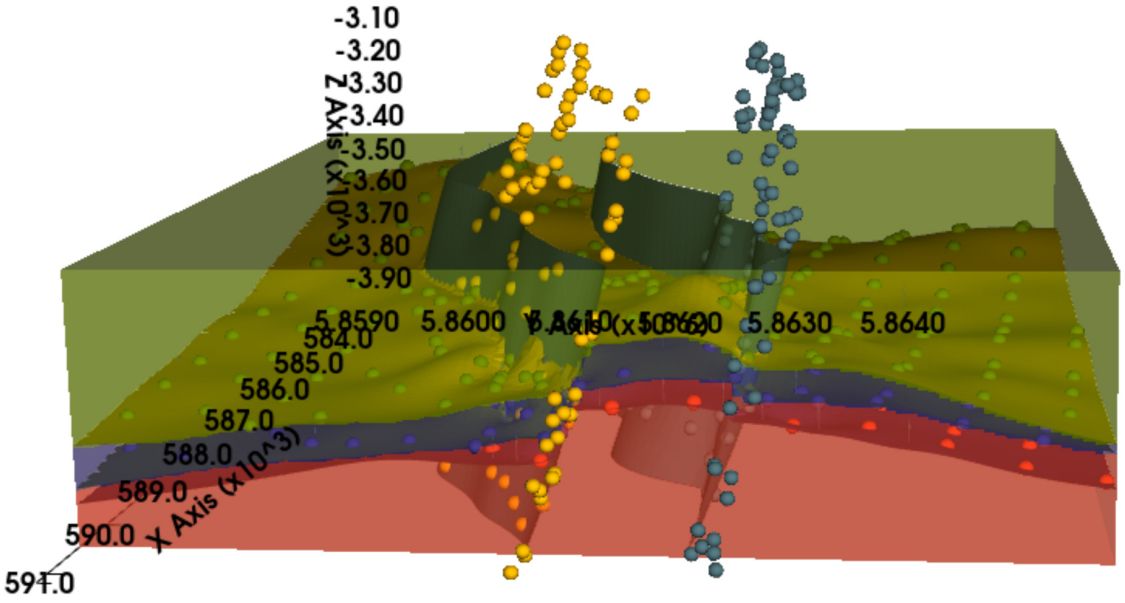

Figure 4-8: End result of the modelling. View on the East side of the model.

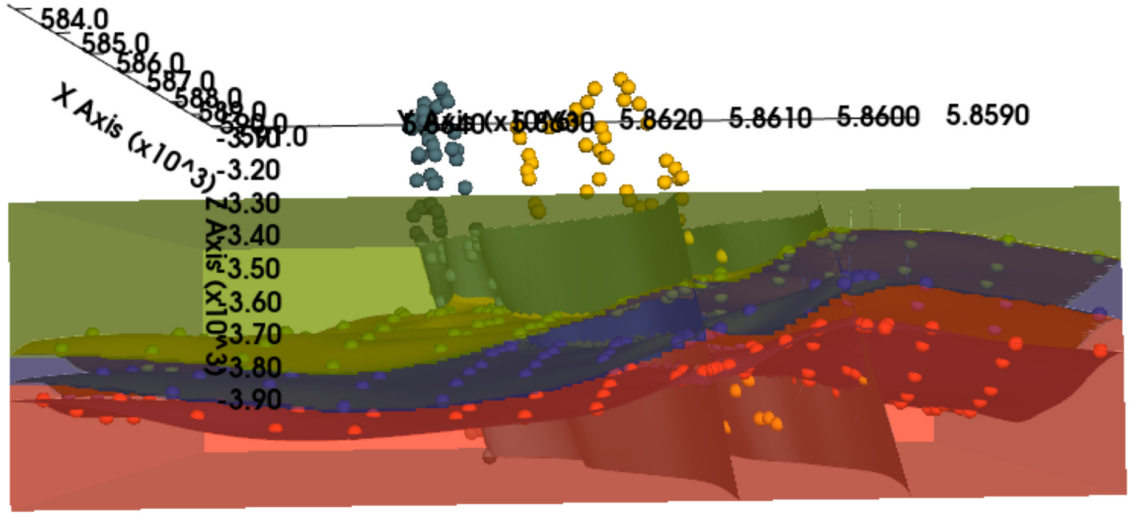

Figure 4-9: End result of the modelling. View on the West side of the model.

Furthermore, the offset caused by the faults can be investigated. For the southern fault, the maximum offset is 90 m and for the northern one, it amounts to 40 m. These offsets are higher than the thicknesses of the reservoir layer, which were determined in section 4-1-1.

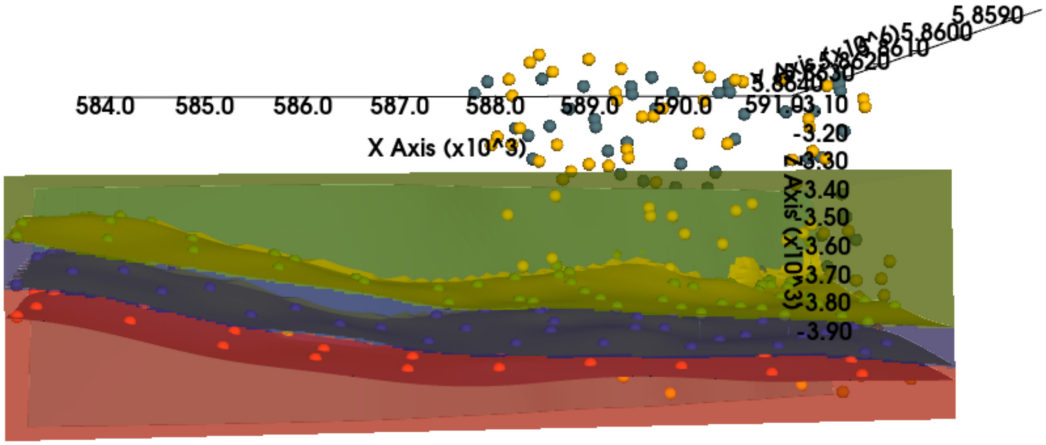

Figure 4-10: End result of the modelling. View on the South side of the model.

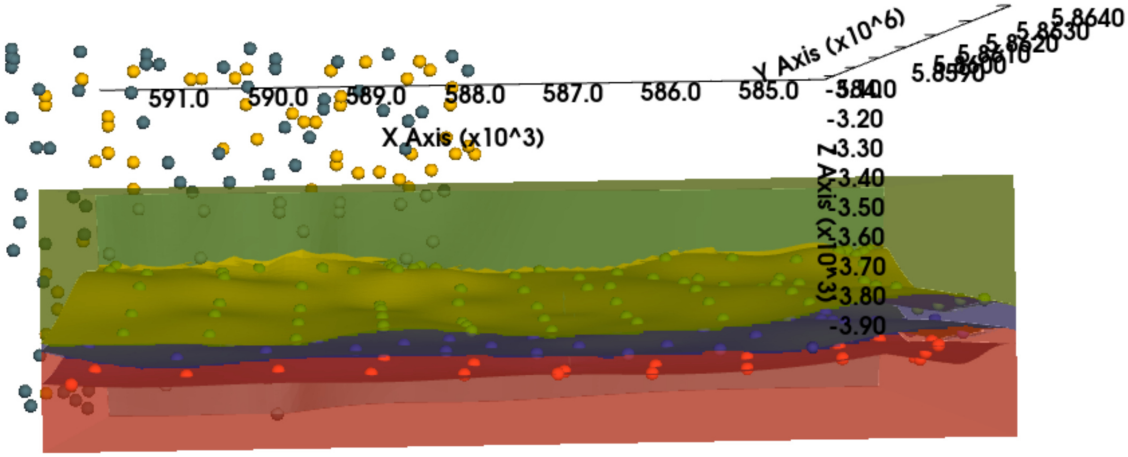

Figure 4-11: End result of the modelling. View on the North side of the model.

4-2-2 Determination of the reservoir thickness

The thicknesses of the Solling and Detfurth formation based on the interface points of the provided model are plotted in figures 4-12 & 4-13. Overall, 66,230 points were used to calculate the thickness distribution of the Solling and 66,274 points for the thickness of the Detfurth. Artefacts on the eastern side of the model area that were caused by the presence of the faults were set to zero for both images and will be filtered out for further calculations. For both, the result of the Solling and the Detfurth formation it is clearly visible that increased thicknesses occur in the area in-between the faults and in the southwestern parts, where the layers are slightly elevated compared to the rest of the model.

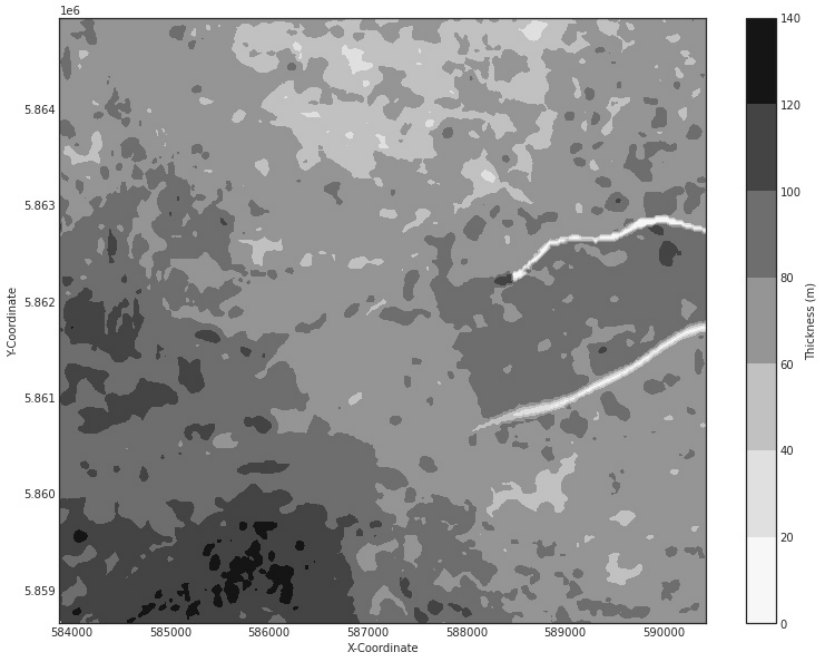

Figure 4-12: Thickness of the Solling formation throughout the model area. The lines with a thickness of 0 m on the right originate from the faults.

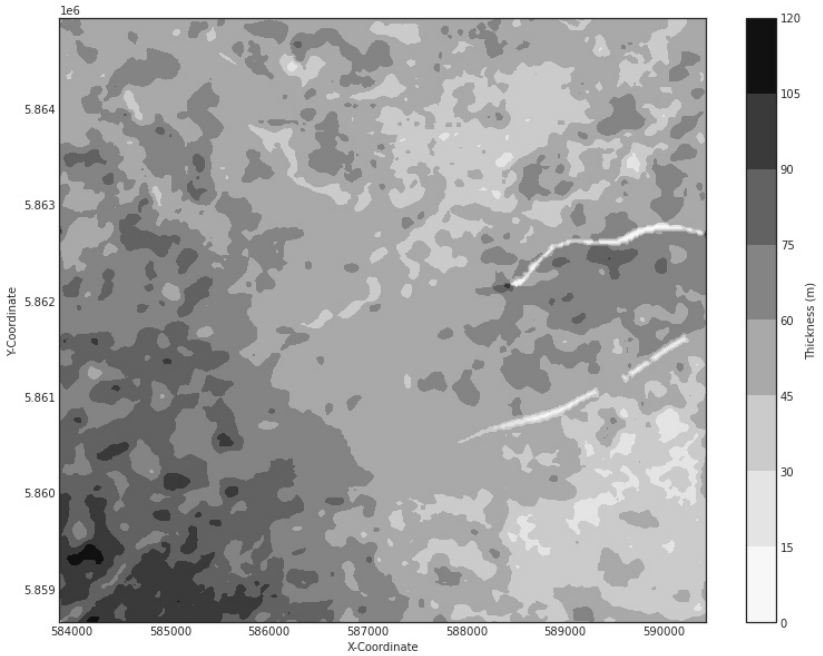

Figure 4-13: Thickness of the Detfurth formation throughout the model area. The lines with a thickness of 0 m on the right originate from the faults.

The maximum thickness of the Solling formation amounts to 143 m. Its mean is 77.97 m with a standard deviation of 16.30 m. Overall more than 69 % of the data points have a thickness

between 60 and 90 m. Figure 4-14 shows a histogram with the distribution of the thicknesses throughout the Solling formation.

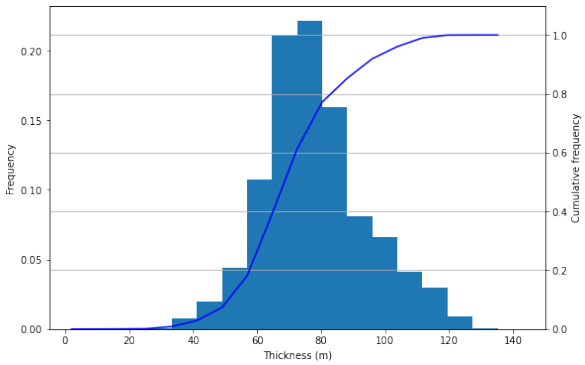

Figure 4-14: Histogram representing the (cumulative) frequency of the thicknesses throughout the Solling formation.

For the Detfurth formation, the thicknesses are much lower. Its maximum thickness is 113 m. The mean is 57.50 m with a standard deviation of 14.92 m. More than 70 % of the points have a thickness within the range of 40-70 m. Figure 4-15 shows a histogram with the distribution of the thicknesses throughout the Detfurth formation.

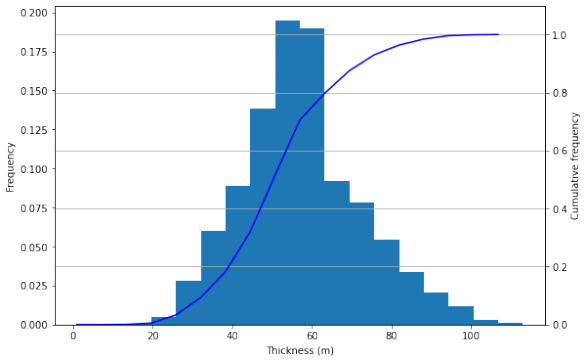

Figure 4-15: Histogram representing the (cumulative) frequency of the thicknesses throughout the Detfurth formation.

Based on the thickness of the entire stratigraphic formations and the results from the logging, the mean thicknesses of the reservoir layers were estimated, including their standard deviations (table 4-1). These thicknesses will be used for further calculations. The thicknesses of the reservoir layers throughout the model area if they behaved equally to the thicknesses of the entire formations are plotted in figures 4-16 - 4-17.

Reservoir Layer	Mean Thickness	Standard Deviation
Solling sand stone	17.37 m	3.63 m
Detfurth sand stone	12.68 m	3.29 m

Table 4-1: Estimated mean thicknesses of the potential reservoir layers; Based on the behaviours of the thicknesses of their corresponding stratigraphic formations.

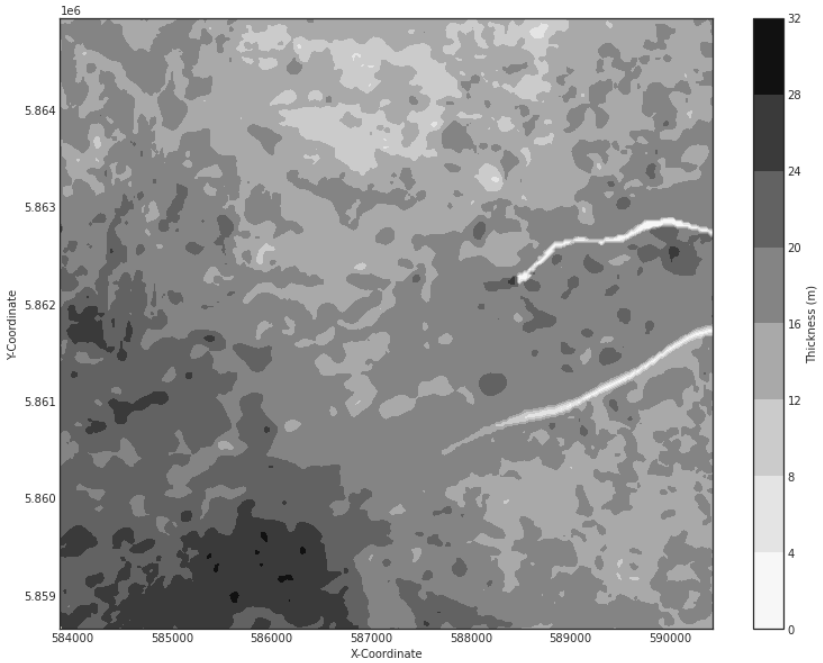

Figure 4-16: Thickness of the Solling layer throughout the model area, if it behaved equally to the thicknesses of the entire Solling formation. The lines with a thickness of 0 m on the right originate from the faults.

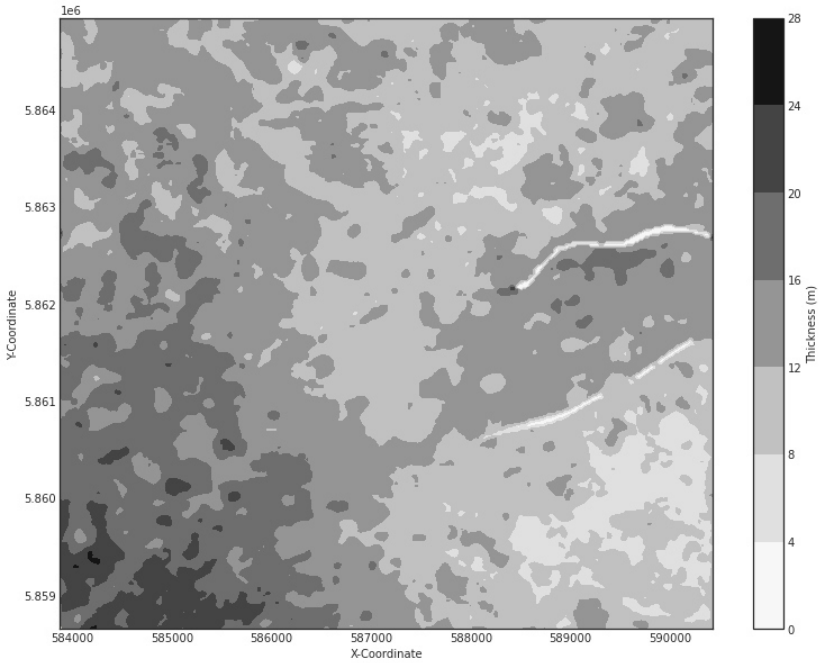

Figure 4-17: Thickness of the Detfurth layer throughout the model area, if it behaved equally to the thicknesses of the entire Detfurth formation. The lines with a thickness of 0 m on the right originate from the faults.

4-3 Lithium-in-place analysis

Based on the results from the logging and the structural model it could be calculated how much lithium is stored in each potential reservoir layer.

The amount of lithium stored in the Solling sandstone ranges from 8,720 t to 18,952 t with a mean of 13,836 t. The min and max values are derived using the error propagation described in section 3-5. For the Detfurth sandstone, the stored amount ranges from 2,508 t to 5,037 t with a mean of 3,773 t. To make these results comparable to other locations, the amounts stored per area are calculated. All results are listed in table 4-2.

Reservoir Layer	Mean Li-content (t)	Min Li-content (t)	Max Li-content (t)
Solling	13,836	8,720	18,952
Detfurth	3,773	2,508	5,037

Table 4-2: calculated lithium contents for each reservoir layer. The min and max values are based on the uncertainties of the input parameters.

4-4 Heat-in-place analysis

The heat-in-place (HIP) is calculated for the potential reservoir layers of the Solling and the Detfurth formations. Again, the input values for the thickness and porosity are based on the outcome from the logging and the modelling. For both potential reservoirs, a range of values is determined, which is based on different specific heat capacities assumed for the aquifer rock. Furthermore, minimum and maximum values are derived, which rely on the outcome of the error propagation. The results are listed in table 4-3.

Reservoir Layer	mean HIP ($GJ\,m^2$)	min HIP ($GJ\,m^2$)	max HIP ($GJ\,m^2$)
Solling	2.59 - 3.04	2.04	3.69
Detfurth	1.85 - 2.19	1.37	2.76

Table 4-3: calculated heat-in-place values for each reservoir layer. The min and max values are based on the uncertainties of the input parameters.

4-5 Doublet calculations

The first doublet calculations will be performed for the case of perfect correlation between the thickness of the reservoir layer and the thickness of the whole Solling formation. Thus, the thickness will take many different values, as the result will be calculated for the entire model area. All other input parameters, including the porosity, which has been derived from the acoustic logging are listed in table 4-4.

Input parameter	Value
Q (L/s)	24*
Φ (%)	6.37 - 11.55
Δ t (a)	30
ρ_w (g cm^{-3})	1**
ρ_r (g cm^{-3})	1.3 - 2.3**
C_w (kJ kg^{-1} K^{-1})	4.12***
C_r (kJ kg^{-1} K^{-1})	0.82 - 1.18***
K_r (W m^{-1} K^{-1})	0.6 - 4.0***

Table 4-4: Values of the input parameters to calculate the distance between injection and production well; Based on Gringarten and Sauty (1975).
*[Agemar et al., 2014]
**[Schön, 2016]
***[Stober and Bucher, 2013]

For the first calculation, the parameters will be chosen in such a way that the resulting distance is maximal. Thus, the properties of the cap rock ρ_r, C_r and K_r are assumed to be minimal. As the factor $\frac{\rho_R c_R}{\rho_w c_w}$, in this case, is smaller than 1, for the porosity also the minimum value will be used. Calculating the distances throughout the entire model area for a reservoir thickness that perfectly correlates with the thickness of the Solling formation results in the following image (fig 4-18):

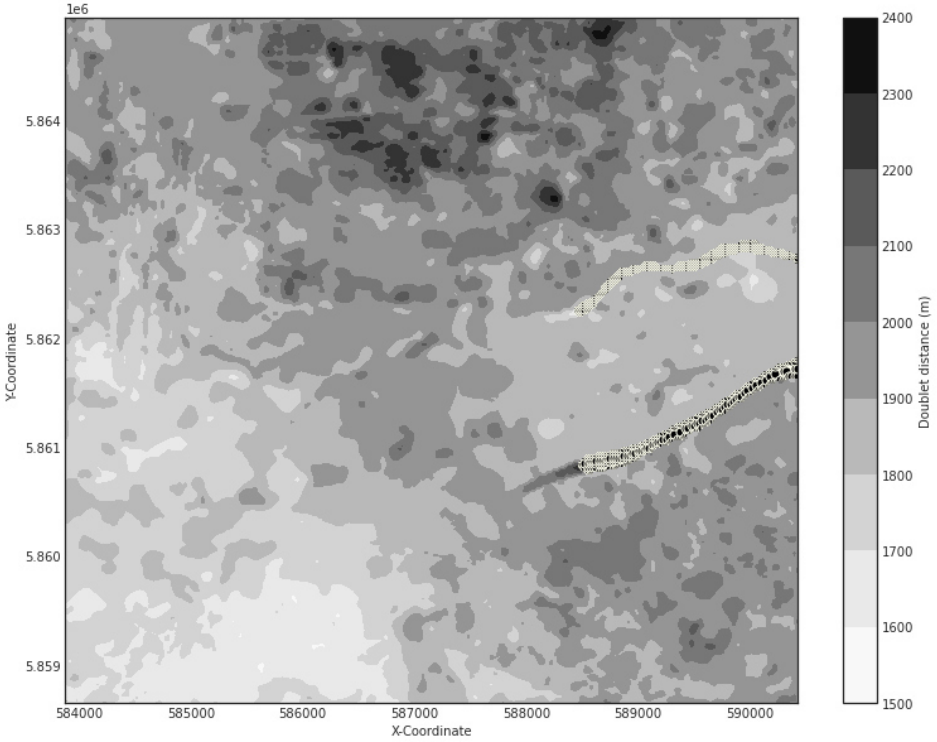

Figure 4-18: Calculated required distances between production and injection well of a geothermal doublet throughout the model area. Minimal values for the input parameters were assumed.

The resulting maximal distances, including a safety factor of 5 % range from 1,520 m to 2,387 m with a mean of 1,899 m. For all other physical parameters being constant, sections of high thickness lead to a low required minimum distance. Thus, the region with the lowest required distance is located in the Southwest of the model area. Also, the region in between the two faults shows low values compared to its surrounding. The highest required distances are located in the North of the model area.

The same procedure is also performed to obtain minimal distances, for the case of maximal values for the properties of the cap rock and the porosity. The resulting distances range from 927 m to 1,242 m with a mean of 1,081 m. The results are visualized in the following image (fig 4-19):

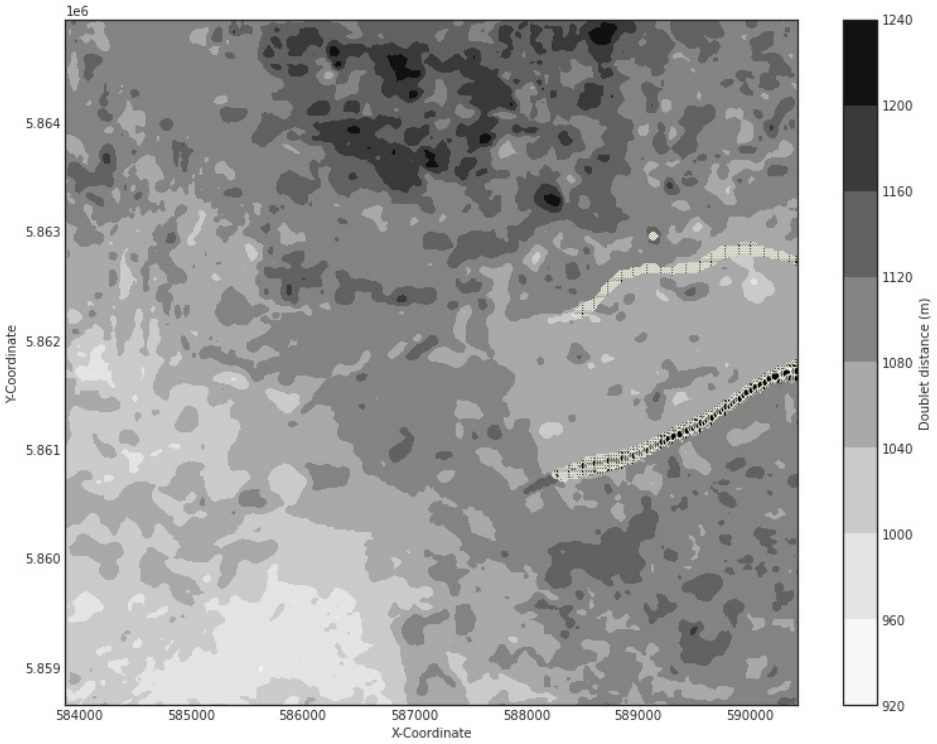

Figure 4-19: Calculated required distances between production and injection well of a geothermal doublet throughout the model area. Maximal values for the input parameters were assumed.

Considering the range of the mean thickness estimated in section 4-3, a range of mean distances, which takes the uncertainty of the thickness into account is calculated. This range is determined to be 1,037 - 2,021 m. Based on these results it is calculated that the total model area could theoretically fit 8 - 28 doublets. Based on formula 3-10 it is calculated that one doublet can produce 540.4 - 660.5 t of LCE per year. This is 3.0 - 3.7 times less than the production of a doublet in the URG. The total annual production of the area for 8 - 28 doublets ranges from 4,323 t to 18,494 t.

4-6 Sensitivity analysis

Regarding the calculations, which target the amount of lithium stored in the reservoir, the porosity contributes more to the uncertainty of the end result, than the thickness. The porosity causes a deviation from the mean result of 28.9 %, while the thickness leads to a deviation of 20.9 %. Due to the linear relationship between the input parameters and the outcome, this percentage deviation corresponds to the coefficient of variation of each input parameter.

For the heat stored in place, the thickness h contributes linearly, while the porosity Φ is contained in the factor γ. Although this relationship is also linear, the contribution of Φ to the end result depends on the densities ρ_w and $_r$ and heat capacities c_w and c_r of the fluid and the aquifer rock. Due to $\frac{\rho_R c_R}{\rho_w c_w}$ being close to 1 for all considered cases, the porosity does not have a big impact on the end result. To quantify this impact, results were calculated while only varying h and Φ within their range of uncertainty and keeping all other values constant. While for h the result deviated by the expected 20.9 % from the mean value, for Φ the maximum deviation was only 3.45 %.

For the calculation of the required distance between the injection and production well not only Φ and h are considered but also the cap rock parameters. These will be viewed as one merged parameter $K_r \rho_r C_r$. For different combinations of Φ, h and $K_r \rho_r C_r$ it is investigated which parameter causes the greatest uncertainty.

This investigation led to the result that the porosity Φ has the lowest impact on the end result. The deviation caused by the uncertainty of the porosity only amounts to 0.2 - 2.1 %. The uncertainty of the thickness h causes a significantly larger deviation of 4.2 - 6.7 %. However, the impact of the cap rock parameters is even bigger. It ranges from 33.0 % to 34.8 %.

Chapter 5

Discussion

In this chapter, the results presented in chapter 4 are evaluated with respect to their uncertainties. Furthermore, they will be compared to values of the Upper Rhine Graben and the North German Basin.

5-1 How much lithium is stored in place?

The first major part of this thesis was to evaluate how much lithium is stored in each of the potential reservoir layers. The lithium content of the Solling sandstone (8,720 - 18,952 t) turned out to be 3.5 to 3.8 times higher than that of the Detfurth sandstone (2,508 - 5,037 t). Such a discrepancy was expected, as the Dethfurt layer has a lower thickness, porosity and lithium concentration.

To make the result comparable with the lithium storage at other locations, the amount of lithium per m^2 is calculated. In the Upper Rhine Graben, the stored lithium amount per m^2 is 0.889 kg [Bundesverband Geothermie, 2021]. This value is 2.83 times higher than the mean amount stored in the Solling sandstone at Horstberg (0.317 $kg\,m^{-2}$). The determined maximum value at Horstberg would still be twice as low and the minimum would even be 4.49 times lower.

For the Detfurth sandstone, the outcome is even less. Its mean lithium content of 0.09 $kg\,m^{-2}$ is 9.88 times lower than that of the Upper Rhine Graben. The maximum value would still be 7.68 times lower and the minimum value even 15.43 times.

The input parameters to derive these results are based on the outcomes of analyzing the log data and the creation of the structural model. The logging consisted of gamma ray and acoustic logging. The measured GR_{API} values from the gamma ray were transformed into shale contents, which can be plotted in comparison to the geological profile of the well (fig 5-1). The largest shaliness of 100 % is obtained from a thin shale layer located at 3,550-3,555 m SSTVD. A shale content of 0 % is calculated for the Halite formation of the Upper Buntsandstein located at 3,500-3,514 m SSTVD. This makes perfect sense, as Halite rocks

usually do not contain any clay minerals [Bonewitz, 2012]. Overall, the clayey sections of the profile match the relatively large shale contents obtained from the gamma ray. A rather unexpected observation is, that also the sandy layers from 3,555-3,613 m SSTVD show this high shale content of 20-30 %. From this, it can be concluded that those sandstones might be more shaly than indicated in the geological profile. Overall, the calculated values appear to be very plausible.

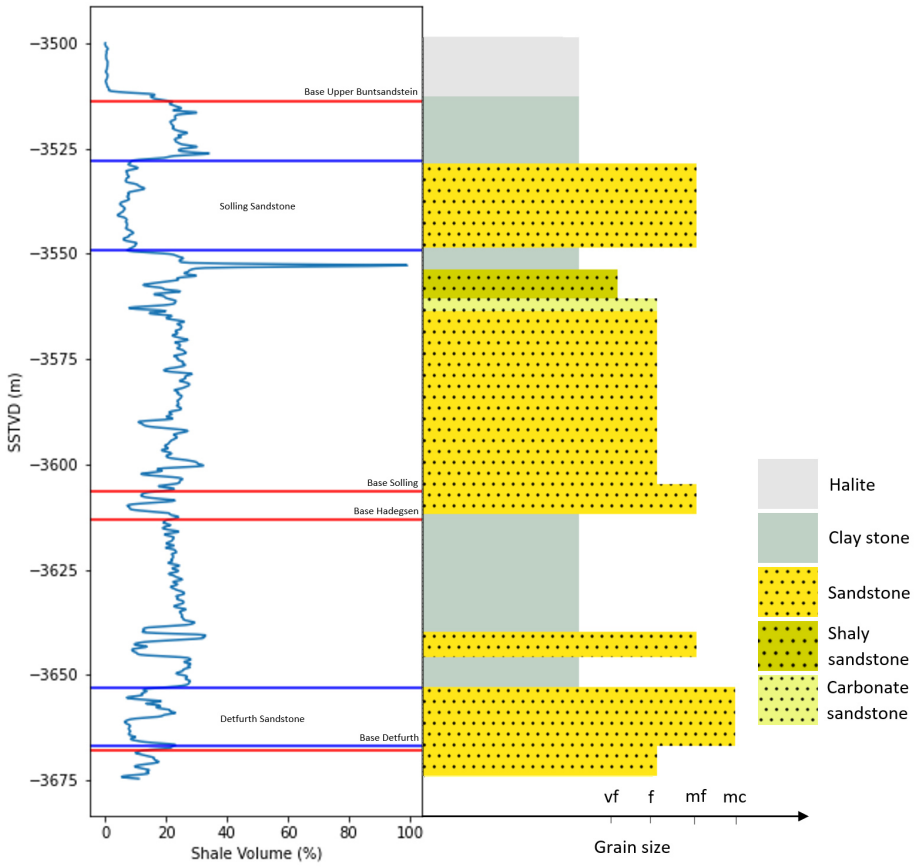

Figure 5-1: Calculated shale contents plotted in comparison to the geological profile of the *Horstberg Z1* well.

The Solling sandstone layer shows a significantly low shale content of 7.7 %. From the vertical extent of this characteristic content, it was derived that the layer thickness amounts to 20.5 m. This value differs from a previous publication by Rühaak et al. (2018), yet, it is supported by the geological profile, which is based on the work of Steuer (2016).

The thickness of the Detfurth sandstone was determined to be 13.7 m. An interesting observation was that the gamma ray data shows a disturbance in the middle of the Detfurth sandstone layer. Thus, with respect to the gamma ray data, the thickness of 13.7 m must be seen as the best case scenario, as the layer might be disrupted.

For both potential reservoir layers, the shale contents of their cap- and bedrock are higher than their own. For the Solling sandstone, this is more distinct than for the Detfurth sandstone, as it is overlaid and underlaid by clay stone layers. Thus, it can be concluded that their

surrounding rocks tend to be less permeable. This could play a big role regarding the two major faults, as for a high offset, they could act as an impermeable barrier.

The acoustic logging was used to investigate the porosity of the reservoir layers based on the work of Wyllie et al. (1959). The resulting porosities of 8.96 % for the Solling sandstone and 7.55 % for the Detfurth are lower than the porosity obtained from the resistivity measurements, which were carried out during the GeneSys project (11 % for Solling and 8.5 % for Detfurth) [Gerling et al., 2015]. Yet, for both potential reservoir layers, those values lie within the ranges of the standard deviations of 2.59 % for the Solling and 1.39 % for the Detfurth. The reason for the differences is likely the two types of measurement. It could be that the resistivity measurements overall are of higher accuracy than the logging. Nevertheless, the log data led to satisfying results.

All results obtained from the logging only represent 1-D data from the location of the *Horstberg Z1* well at specific depths. Throughout the entire reservoir area, the obtained parameter might vary heavily. Unfortunately, no other data, e.g. from other well locations was available. Thus, all further calculations must rely on the parameter ranges obtained from the logging.

To obtain information about the reservoir in 3-D space, a structural model was recreated in GemPy. The biggest challenge of the modelling proved to be the "out-pinching" character of the two faults, meaning that they have a large offset at the eastern part of the model, which disappears towards the center. The modelling of this type of fault turned out to be very difficult in Gempy, as it is not that easy to let a fault completely disappear at a certain point. Instead, the impact of the fault must be minimized using additional points and orientations. Despite all efforts, the final result still also contains fault artefacts on the western side of the model (fig 4-9).

From the resulting model, two major conclusions could be drawn. Firstly, it has been observed that the northern part of the model has lower thicknesses than the southern part of the model. Yet, the layer's orientation can generally be assumed as horizontal. This assumption is an important pre-condition for the lithium and heat in place analysis, as well as for the doublet calculations.

Secondly, the offset caused by both faults is bigger than the thickness of the reservoir layers. Thus, the reservoir will be interrupted entirely at the location of the faults. From the results of the logging, it could be concluded that the cap- and bedrock of the reservoir layers contain high volumes of shale. This could indicate that those layers are of low permeability. If this is the case, the fault acts as an impermeable barrier for the fluid stored inside the reservoir. This would also have consequences for the design of a geothermal doublet, as then the injection and production wells of one doublet should not be placed on different sides of this barrier. The reason for that is that the injection is supposed to keep the pressure of the reservoir in an equilibrium, which would be disturbed by the presence of the fault. On one side of the fault, the pressure would get less due to the production and on the other one, it would get bigger because of the injection. Because of the presence of the impermeable barrier, this imbalance could not easily be equalized. Based on the outcome from the logging and the modelling, the thicknesses of the reservoir layers throughout the model area have been investigated. These thicknesses were then used to calculate the lithium and heat stored in those reservoir layers.

Comparing the parameters, which were used to calculate the lithium stored in place at Horstberg with the conditions at the Upper Rhine Graben, the reasons for the large dif-

ference in the stored quantity can be determined. The porosity of Buntsandstein reservoirs at the Upper Rhine Graben is 7-12 %, which is similar to that of the Solling layer at Horstberg (6.37 - 11.55 %) [Jodocy and Stober, 2011]. Also the lithium concentration of the stored fluid is similar at both locations (Horstberg (Solling): 204 mg/l, URG: 120-220 mg/l) [Bundesverband Geothermie, 2021]. Thus, the lower lithium amount of the Solling layer can mainly be traced back to the thickness of the reservoir layer. For the Detfurth layer, the thickness is even lower than that of the Solling layer. However, also the lower porosity and lithium concentration contribute to the low result.

5-2 How much heat is stored in place?

Secondly, besides the amount of lithium stored in the reservoir, also the heat-in-place was investigated. It was found that the heat stored in the Solling layer is up to 1.5 times higher than that of the Detfurth layer. To be able to classify the results better, they are compared to other values from the Buntsandstein in the North German Basin.

Generally, the North German Basin is one of three main areas in Germany for potential geothermal lithium exploration (fig 5-2). The Buntsandstein particularly represents an attractive stratigraphic formation, as it is widespread throughout the whole basin and has thicknesses up to several hundred meters. Furthermore, it is often found at suitable depths to explore geothermal energy [Reinhold et al., 2011]. The mean heat-in-place of the Middle Buntsandstein in the North German basin, excluding areas of no potential, is 2.46 $\mathrm{GJ\,m^{-2}}$ [Frick et al., 2022]. This is slightly lower than the calculated mean value of the Solling sandstone (2.59 - 3.04 $\mathrm{GJ\,m^{-2}}$) and moderately higher than the mean value of the Detfurth sandstone (1.85 - 2.19 $\mathrm{GJ\,m^{-2}}$). Taking into account that the results for the potential reservoir layers considered in this thesis are only shares of the entire Middle Buntsandstein, the stored heat in those layers can overall be assessed as high.

5-3 How much lithium could be extracted?

The third part of this thesis targeted the design of a potential geothermal doublet. Due to the low amount of lithium stored in the Detfurth layer, the calculations focused on the Solling layer only. The calculations are performed on the theoretical assumption that the production rate is equal to that of a Middle Buntsandstein reservoir in the Upper Rhine Graben. The goal of this investigation is to assess if reservoirs with properties similar to those at Horstberg, but with a higher production rate could potentially be used for the geothermal exploration of lithium.

For potential geothermal doublets, it was calculated that the mean required distance between injection and production well is in the range of 1,037 - 2,021 m. This outcome depends on many different parameters, including the properties of the cap rock. Overall, this distance is quite high, which again results from the low thickness of the reservoir. For a reservoir with higher thickness the zone of injected water does not expand as fast in the lateral direction as for a reservoir of low thickness [Gringarten and Sauty, 1975]. Thus, for a reservoir of lower thickness, the distance between injection and production well must be larger. Such big distances could cause a problem regarding the need to maintain the pressure inside the

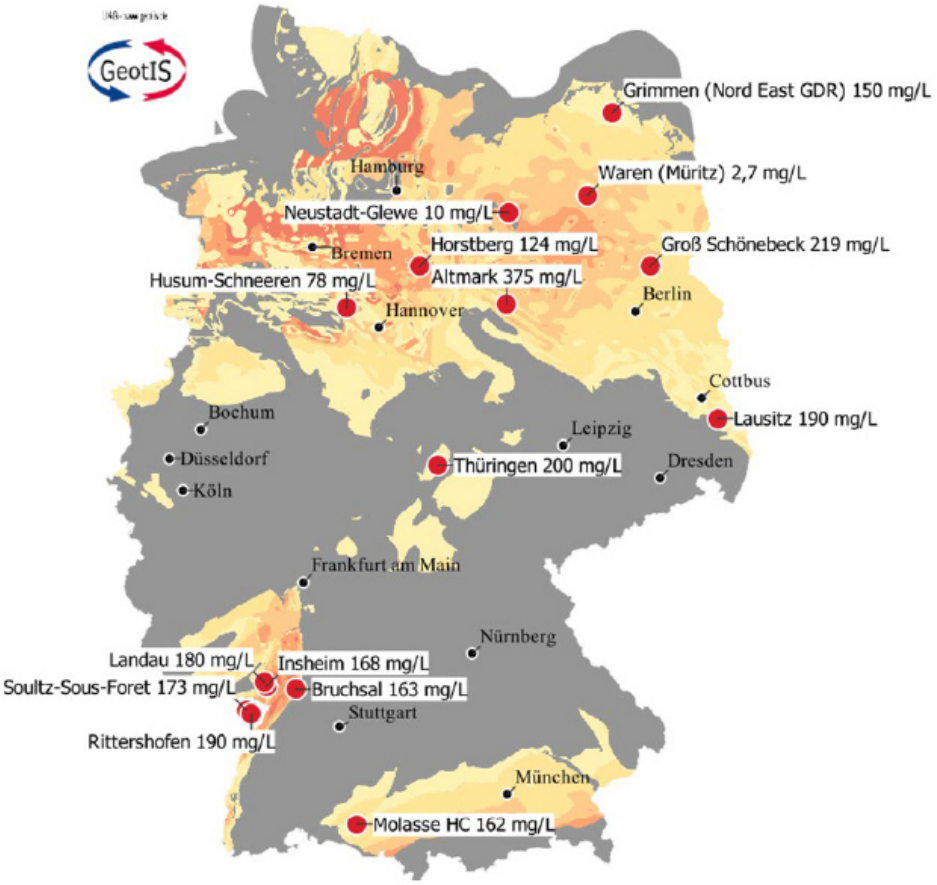

Figure 5-2: Areas in Germany with potential for geothermal lithium production; Based on Agemar, 2014; [Alms et al., 2022]

reservoir at a constant level. Furthermore, the choice of location would be more limited than for shorter required distances.

Based on the mean required distance, it was calculated that the model area could fit 8-28 doublets with an annual lithium production of 4,323 - 18,494 t. This value is very unrealistic, as it would exceed the amount of lithium stored in the area within 1-4 years. Thus, for this scenario to work out, constant recharge of the reservoir would be required. It is more realistic to firstly concentrate on the design of one single doublet.

From the previous results, it can be concluded that the best location for a doublet would be the southwestern part of the model, as this is the area with the highest thickness. High thicknesses would be beneficial, as based on the assumption of homogeneous porosity and lithium concentration, the amount stored lithium content would be bigger than elsewhere. Also, the distance of the production and injection well would be smaller than for low thicknesses. Furthermore, this location would be unaffected by the presence of the faults. So far, the lithium concentration and porosity have been assumed to be constant throughout the whole reservoir. For the design of a doublet in the southwestern part of the model, these parameters and their lateral variation would have to be investigated more closely.

The annual production of LCE for one doublet has been determined to be 540.4 -

660.5 t. This result is 3.0 - 3.7 times lower than the estimated production of the Upper Rhine Graben (2,000 t LCE/a; [Bundesverband Geothermie, 2021]). This can be explained by the fact that the production rate in the Upper Rhine Graben is up to 80 l/s. [Bundesverband Geothermie, 2021]. However, the calculated LCE production would still be enough to produce up to 6600 car batteries per year, which could be economically profitable.

5-4 Which parameters have the highest impact on the results?

Finally, it is analysed which parameters that include a range of uncertainty have the biggest impact on the uncertainty of the final results. It could be concluded that due to the larger range of uncertainty, the porosity is the more sensitive parameter regarding the "Lithium-in-place analysis". Yet, due to the impact of the densities and heat capacities, the thickness is more sensitive regarding the calculation of the "Heat-in-place". The distance between injection and production well of a doublet is affected more by the thickness than by the porosity, yet the largest spread is caused by the different assumed cap rock parameters. To reduce the uncertainty of each result, it is advisable to focus on those parameters that affect the outcome of each calculation the most.

5-5 Error discussion

Regarding the lithium- and heat-in-place analysis, the calculation is based on the assumption that the entire reservoir is saturated. Furthermore, the porosities and thicknesses used for the calculation are based on data from only one location throughout the area, which makes it impossible to take lateral variations of these parameters into account. The same accounts for the lithium concentration of the stored fluid. For the concentration, furthermore, no information on the uncertainties of the measurements was available. The rather arbitrarily assumed measurement error of 10 % represents another error source, which could be limited if measurements from more locations were available.

Concerning the doublet calculations, many input parameters were chosen based on data from the literature. These might deviate from the real parameters at the reservoir location. Furthermore, the distance between the injection and production well is always a trade-off between avoiding a thermal breakthrough and minimizing the drawdown pressure difference between the points of injection and production [Wellmann et al., 2010]. The calculation in this thesis only focused on the distance required to avoid a thermal breakthrough.

5-6 Conclusion

Overall, it can be concluded that the conditions for geothermal lithium exploration at Horstberg are suboptimal. The stored lithium in place is much lower than at the Upper Rhine Graben. This is mainly caused by the low thickness of the reservoir layers. Furthermore, the exploration would be limited to the low production rates and large required distances between the injection and production well of a geothermal doublet. These large required distances can again be drawn back to the low thickness of the reservoir.

Nevertheless, this thesis gave a good example of how to assess a potential geothermal lithium reservoir of the Middle Buntsandstein in the North German Basin. Similar methods could be used to evaluate potential reservoirs at other locations.

Chapter 6

Summary & Outlook

In this thesis, it was evaluated how much lithium is stored in two potential reservoir layers of the Middle Buntsandstein. Furthermore, the required distance between the production and injection well for a geothermal doublet was evaluated for a production rate similar to that of a Buntsandstein reservoir in the Upper Rhine Graben.

It could be confirmed that regarding the porosity, thickness and Lithium content, the sandstone layer of the Solling has the more promising properties to be a geothermal lithium reservoir, than the Detfurth. In comparison to reservoirs in the Upper Rhine Graben, it was found that the average Lithium content per area stored in the Solling sandstone at Horstberg is 2 - 4.5 times lower. This is mainly due to the low thickness of the Solling sandstone layer.

The doublet calculation was a theoretical investigation, which showed that even with a production rate from a Middle Buntsandstein reservoir of similar porosity, the outcome would still be lower than in the Upper Rhine Graben. This can be drawn back to the fact that other reservoirs in the Upper Rhine Graben have even higher production rates than the rate assumed for the theoretical calculation.

In the future, similar investigations should be carried out at other locations in Germany and Europe to evaluate the overall capability to become more independent of imports and to increase the sustainability of lithium production. As shown in figure 5-2, the potential of lithium exploration from geothermal sources in Northern Germany is quite high. Many locations show high thermal gradients and lithium concentrations. Production of geothermal lithium in the North German Basin would be particularly attractive, as it is also logistically very beneficial. For example, the automotive group *Volkswagen* has announced to build a factory to produce lithium-ion batteries in the town of Salzgitter in Lower Saxony [Volkswagen AG, 2020].

For each location investigated in the future, it must be evaluated, whether the amount of stored lithium and the potential production value are suitable to create economic profit. Therefore, it will be of high importance to reduce the uncertainties of the calculations. To achieve this, the amount of provided and acquired data is decisive. Especially to investigate lateral variations of the parameters, it would be beneficial to have data from many different locations.

Another aspect that has to be considered when investigating the exploration of lithium from geothermal reservoirs is the recharge of the reservoir. This recharge could occur through enrichment of the re-injected, lithium-depleted water or due to a supply of new lithium-enriched thermal fluid. For the enrichment, the presence of clay minerals might play a big role, while for the supply of new fluids, the flow inside the reservoir, the origin of the fluid and the lateral extent of the reservoir should be investigated [Vine and Dooley, 1980]. The flow would also be of importance for the design of a doublet system, as the injection and production well should be oriented, such that the flow of the fluid counteracts the flow of the re-injected water towards the production well [Gringarten and Sauty, 1975].

Bibliography

[Agemar et al., 2014] Agemar, T., Weber, J., and Schulz, R. (2014). Deep geothermal energy production in germany. *Energies*, 7(7):4397–4416.

[Alms et al., 2022] Alms, K., Jagert, F., Blömer, J., and Gehrke, I. (2022). Co-production of geothermal energy and lithium from geothermal waters.

[Baldschuhn et al., 2001] Baldschuhn, R., Binot, F., Fleig, S., and Kockel, F. (2001). Geotektonischer atlas von nordwest-deutschland und dem-deutschen nordsee-sektor.

[BGR, 2008] BGR (2008). Bgr - genesys horstberg.

[Bonewitz, 2012] Bonewitz, R. L. (2012). *Rocks and minerals*. DK Smithsonian nature guide. DK Publishing, London and New York, 1st american ed. edition.

[Brink, 2005] Brink, H.-J. (2005). The evolution of the north german basin and the metamorphism of the lower crust. *International Journal of Earth Sciences*, 94(5):1103–1116.

[Bundesverband Geothermie, 2020] Bundesverband Geothermie (2020). Becken, norddeutsches.

[Bundesverband Geothermie, 2021] Bundesverband Geothermie (2021). Lithium. https://www.geothermie.de/bibliothek/lexikon-der-geothermie/l/lithium.html (6/28/2022).

[Ellis and Singer, 2007] Ellis, D. V. and Singer, J. M. (2007). *Well logging for earth scientists*, volume 692. Springer.

[Franz et al., 2015] Franz, M., Wolfgramm, M., Barth, G., Nowak, K., Zimmermann, J., Budach, I., and Thorwart, K. (2015). Verbundprojekt: Identifikation hydraulisch geeigneter bereiche innerhalb der mesozoischen sandsteinaquifere in norddeutschland [r&d project: Hydraulic properties of mesozoic sandstone aquifers of north germany]. *Forschungsvorhaben, Dokumentation, Schlussbericht TU Bergakademie Freiberg, Freiberg, Germany*.

[Frick et al., 2022] Frick, M., Kranz, S., Norden, B., Bruhn, D., and Fuchs, S. (2022). Geothermal resources and ates potential of mesozoic reservoirs in the north german basin. *Energies*, 15(6):1980.

[GemPy.org, 2022] GemPy.org (02.08.2022). Open-source 3d structural geomodeling — gempy. https://www.gempy.org/ (08/02/2022).

[Gerling et al., 2015] Gerling, J. P., Tischner, T., Kosinowski, M., and Bräuer, V. (2015). Erdwärmegewinnung mittels generierter geothermischer systeme (genesys).

[Gringarten and Sauty, 1975] Gringarten, A. and Sauty, J. (1975). A theoretical study of heat extraction from aquifers with uniform regional flow. *Journal of geophysical research*, 80(35):4956–4962.

[Gringarten, 1978] Gringarten, A. C. (1978). Reservoir lifetime and heat recovery factor in geothermal aquifers used for urban heating. *Pure and applied geophysics*, 117(1):297–308.

[IEA, 2020] IEA (2020). Global ev outlook 2020. URL: https://www. iea. org/reports/global-ev-outlook-2020 (6/30/2022).

[Jerez et al., 2021] Jerez, B., Garcés, I., and Torres, R. (2021). Lithium extractivism and water injustices in the salar de atacama, chile: The colonial shadow of green electromobility. *Political Geography*, 87:102382.

[Jodocy and Stober, 2011] Jodocy, M. and Stober, I. (2011). Porositäten und permeabilitäten im oberrheingraben und südwestdeutschen molassebecken. *Erdöl, Erdgas, Kohle*, 127(1):20.

[Jung et al., 2002] Jung, R., Röhling, S., Ochmann, N., Rogge, S., Schellschmidt, R., Schulz, R., and Thielemann, T. (2002). Abschätzung des technischen potenzials der geothermischen stromerzeugung und der geothermischen kraft-wärme-kopplung (kwk) in deutschland.

[Muffler and Cataldi, 1978] Muffler, P. and Cataldi, R. (1978). Methods for regional assessment of geothermal resources. *Geothermics*, 7(2-4):53–89.

[Reinhold et al., 2011] Reinhold, K., Müller, C., and Riesenberg, C. (2011). Informationssystem speichergesteine für den standort deutschland-synthese. *Bundesanstalt für Geowissenschaften und Rohstoffe, Berlin/Hannover*.

[Röhling, 2014] Röhling, H.-G. (2014). Der buntsandstein im norddeutschen becken–regionale besonderheiten. *Schriftenreihe der Deutschen Gesellschaft für Geowissenschaften*, pages 269–384.

[Sanjuan et al., 2022] Sanjuan, B., Gourcerol, B., Millot, R., Rettenmaier, D., Jeandel, E., and Rombaut, A. (2022). Lithium-rich geothermal brines in europe: An up-date about geochemical characteristics and implications for potential li resources. *Geothermics*, 101:102385.

[Schanz Jr, 1979] Schanz Jr, J. J. (1979). Problems and opportunities in adapting us geological survey terminology to energy resources. In *Methods and Models for Assessing Energy Resources*, page 90. Elsevier.

[Schön, 2016] Schön, J. H. (2016). Density. In Schön, J., editor, *Physical properties of rocks*, volume 65 of *Developments in Petroleum Science*, pages 109–118. Elsevier, Amsterdam, Netherlands.

[Scott, 2009] Scott, D. W. (2009). Sturges' rule. *Wiley Interdisciplinary Reviews: Computational Statistics*, 1(3):303–306.

[Sobol, 2001] Sobol, I. M. (2001). Global sensitivity indices for nonlinear mathematical models and their monte carlo estimates. *Mathematics and computers in simulation*, 55(1-3):271–280.

[Steuer, 2016] Steuer, S. (2016). Erstellung eines digitalen 3d-lithologiemodells des mittleren buntsandstein im bereich der bohrung horstberg z1.

[Stober and Bucher, 2013] Stober, I. and Bucher, K. (2013). Geothermal energy. *Germany: Springer-Verlag Berlin Heidelberg. doi*, 10:978–3.

[Stober et al., 2014] Stober, I., Wolfgramm, M., and Birner, J. (2014). Hydrochemie der tiefenwässer in deutschland—hydrochemistry of deep waters in germany. *Z Geol Wiss*, 41(42):5–6.

[Szabó et al., 2014] Szabó, N. P., Dobróka, M., Turai, E., and Szűcs, P. (2014). Factor analysis of borehole logs for evaluating formation shaliness: a hydrogeophysical application for groundwater studies. *Hydrogeology Journal*, 22(3):511–526.

[Tabelin et al., 2021] Tabelin, C. B., Dallas, J., Casanova, S., Pelech, T., Bournival, G., Saydam, S., and Canbulat, I. (2021). Towards a low-carbon society: A review of lithium resource availability, challenges and innovations in mining, extraction and recycling, and future perspectives. *Minerals Engineering*, 163:106743.

[Tearpock and Bischke, 2002] Tearpock, D. J. and Bischke, R. E. (2002). *Applied subsurface geological mapping with structural methods*. Pearson Education.

[Tischner, 2018] Tischner, T. (2018). BGR - Geothermie - Geothermie-Bohrung Horstberg Z1.

[UnLimited, 2022] UnLimited (2022). Projektbeschreibung. https://www.geothermal-lithium.org/projektbeschreibung (7/30/2022).

[U.S. Geological Survey, 2022] U.S. Geological Survey (2022). Mineral commodity summaries 2022. page 101.

[Vine and Dooley, 1980] Vine, J. D. and Dooley, J. (1980). *Where on earth is all the lithium*. US Department of the Interior, Geological Survey.

[Volkswagen AG, 2020] Volkswagen AG (2020). Batterie-standort salzgitter. https://www.volkswagenag.com/de/news/2020/05/Volkswagen_invests_in_battery_operations_at_Salzgitter.html (03.08.2022).

[W Rühaak et al., 2018] W Rühaak, R Jatho, A Hassanzadegan, W Hübner, and T Tischner (2018). Forschungsbohrung horstberg z1: Aktuelle arbeiten und untersuchungen zur geothermischen nutzung gering durchlässiger sedimentgesteine im norddeutschen becken.

[Warren, 2021] Warren, P. (2021). Techno-economic analysis of lithium extraction from geothermal brines. Technical report, National Renewable Energy Lab.(NREL), Golden, CO (United States).

[Wellmann et al., 2010] Wellmann, J. F., Horowitz, F., Ricard, L., and Regenauer-Lieb, K. (2010). Estimates of sustainable pumping in hot sedimentary aquifers: Theoretical considerations, numerical simulations and their application to resource mapping. In *Aust Geotherm Conf*, pages 215–221.

[Werbos, 1982] Werbos, P. J. (1982). Applications of advances in nonlinear sensitivity analysis. In *System modeling and optimization*, pages 762–770. Springer.

Appendix A

Gempy Code

```
#!/usr/bin/env python
# coding: utf-8

# In[1]:


import gempy as gp
import pandas as pd
import geopandas as gpd
import numpy as np
import matplotlib.pyplot as plt
import os


# In[2]:


data_path = 'C:/Users/User/Desktop/Fraunhofer/Masterarbeit/Model'

# import horizons
df_Basis_so = pd.read_csv(data_path + '/Export_Petrel/Horizonte/Basis_so_pd.txt', delimiter=' ',
    index_col=False).iloc[::502, :]
df_Basis_so['formation'] = 'Basis_so'
# adding additional points
df_Basis_so.loc[len(df_Basis_so.index)] = [590375, 5861675, -3662, 'Basis_so']
df_Basis_so.loc[len(df_Basis_so.index)] = [590400, 5861825, -3553, 'Basis_so']
df_Basis_so.loc[len(df_Basis_so.index)] = [584499, 5860006, -3481, 'Basis_so']
df_Basis_so.loc[len(df_Basis_so.index)] = [590100, 5861850, -3539, 'Basis_so']
df_Basis_so.loc[len(df_Basis_so.index)] = [589500, 5861600, -3552, 'Basis_so']
df_Basis_so.loc[len(df_Basis_so.index)] = [589400, 5861150, -3671, 'Basis_so']
df_Basis_so.loc[len(df_Basis_so.index)] = [589200, 5862725, -3605, 'Basis_so']
df_Basis_so.loc[len(df_Basis_so.index)] = [590300, 5863200, -3602, 'Basis_so']

# adding additional points
df_Basis_so2 = pd.read_csv(data_path + '/Filtered_data/df_in_so_samples.csv',  index_col=False)
df_Basis_so = pd.concat([df_Basis_so, df_Basis_so2
                        ]).reset_index().drop('index', axis=1)


df_Basis_smS = pd.read_csv(data_path + '/Export_Petrel/Horizonte/Basis_smS_pd.txt', delimiter=' ',
    index_col=False).iloc[::501, :]
df_Basis_smS['formation'] = 'Basis_smS'
# adding additional points
df_Basis_smS.loc[len(df_Basis_smS.index)] = [590361, 5861604, -3755, 'Basis_smS']
df_Basis_smS.loc[len(df_Basis_smS.index)] = [590416, 5861755, -3647, 'Basis_smS']
df_Basis_smS.loc[len(df_Basis_smS.index)] = [590404, 5862801, -3668, 'Basis_smS']
df_Basis_smS.loc[len(df_Basis_smS.index)] = [590398, 5862705, -3625, 'Basis_smS']
df_Basis_smS.loc[len(df_Basis_smS.index)] = [590439, 5861100, -3772, 'Basis_smS']
df_Basis_smS.loc[len(df_Basis_smS.index)] = [590439, 5861537, -3753, 'Basis_smS']
df_Basis_smS.loc[len(df_Basis_smS.index)] = [590423, 5861635, -3741, 'Basis_smS']
df_Basis_smS.loc[len(df_Basis_smS.index)] = [589850, 5861475, -3641, 'Basis_smS']
df_Basis_smS.loc[len(df_Basis_smS.index)] = [589975, 5861350, -3744, 'Basis_smS']
df_Basis_smS.loc[len(df_Basis_smS.index)] = [589600, 5861050, -3750, 'Basis_smS']
df_Basis_smS.loc[len(df_Basis_smS.index)] = [590300, 5863200, -3684, 'Basis_smS']
df_Basis_smS.loc[len(df_Basis_smS.index)] = [590400, 5862900, -3671, 'Basis_smS']

# adding additional points
```

```
df_Basis_smS2 = pd.read_csv(data_path + '/Filtered_data/df_in_smS_samples.csv',  index_col=False)
df_Basis_smS = pd.concat([df_Basis_smS, df_Basis_smS2
                        ]).reset_index().drop('index', axis=1)


df_Basis_smD = pd.read_csv(data_path + '/Export_Petrel/Horizonte/Basis_smD_pd.txt', delimiter=' ',
    index_col=False).iloc[::500, :]
df_Basis_smD['formation'] = 'Basis_smD'
# adding additional points
df_Basis_smD.loc[len(df_Basis_smD.index)] = [590361, 5861494, -3808, 'Basis_smD']
df_Basis_smD.loc[len(df_Basis_smD.index)] = [583936, 5860470, -3693, 'Basis_smD']
df_Basis_smD.loc[len(df_Basis_smD.index)] = [590400, 5861950, -3691, 'Basis_smD']
df_Basis_smD.loc[len(df_Basis_smD.index)] = [590400, 5861675, -3709, 'Basis_smD']
df_Basis_smD.loc[len(df_Basis_smD.index)] = [589525, 5861000, -3801, 'Basis_smD']
df_Basis_smD.loc[len(df_Basis_smD.index)] = [589350, 5860880, -3801, 'Basis_smD']

# adding additional points
df_Basis_smD2 = pd.read_csv(data_path + '/Filtered_data/df_in_smD_samples.csv',  index_col=False)
df_Basis_smD = pd.concat([df_Basis_smD, df_Basis_smD2
                        ]).reset_index().drop('index', axis=1)

# import faults
df_Abschiebung = pd.read_csv(data_path + '/Export_Petrel/St rungen/Abschiebung_pd.txt', delimiter='
    ', index_col=False)
df_Abschiebung = df_Abschiebung[(df_Abschiebung['Z']<=-3000) & (df_Abschiebung['Z']>=-4000)].sample(
    n=100, random_state=1)
df_Abschiebung['formation'] = 'Abschiebung'

df_St rung = pd.read_csv(data_path + '/Export_Petrel/St rungen/St rung_pd.txt', delimiter=' ',
    index_col=False)
df_St rung = df_St rung[(df_St rung['Z']<=-3000) & (df_St rung['Z']>=-4000)].sample(n=100,
    random_state=1)
df_St rung['formation'] = 'Stoerung'

# adding additional points
df_Abschiebung.loc[len(df_Abschiebung.index)] = [584763, 5860923, -3753, 'Abschiebung']
df_St rung.loc[len(df_St rung.index)] = [585744, 5859768, -3777, 'Stoerung']


# In[3]:


# merging all horizons
df_Basis = pd.concat([df_Basis_so,
                      df_Basis_smS,
                      df_Basis_smD])


# In[4]:


# merging horizons and faults
surface_df = pd.concat([df_Basis,
                        df_Abschiebung,
                        df_St rung
                       ]).reset_index().drop('index', axis=1)


# In[5]:


# create geodataframe
Basis_df = surface_df[(surface_df['formation'].isin(['Basis_smD',
                                                     'Basis_smS',
                                                     'Basis_so'
                                                    ]))]

Basis_df_gdf = gpd.GeoDataFrame(geometry=gpd.points_from_xy(x=Basis_df['X'],
                                                            y=Basis_df['Y']),
                                data=Basis_df)


# In[6]:


surface_df_gdf = gpd.GeoDataFrame(geometry=gpd.points_from_xy(x=surface_df['X'],
                                                              y=surface_df['Y']),
                                  data=surface_df)


# In[7]:


# load orientations
df_orientation = pd.read_csv(data_path + '/orientation.csv', delimiter=';')
df_orientation = df_orientation[df_orientation['formation'].isin(('Abschiebung', 'Stoerung',
    'Basis_so', 'Basis_smD', 'Basis_smS'
                                                                  ))].reset_index().drop('index',
                                                                      axis=1)
```

```
# In[8]:


# create model
geo_model = gp.create_model('Model1')

# In[9]:


# set boundaries and resolution
gp.init_data(geo_model, [583800, 590500, 5858500, 5865000, -4000, -3400], [100, 100, 100],
             surface_points_df=surface_df,
             orientations_df=df_orientation,
             default_values=True)

# In[10]:


# show surfaces

geo_model.surfaces

# In[11]:


#  classify surfaces

gp.map_stack_to_surfaces(geo_model,
                         {
                             'Stoerung1' : ('Abschiebung'),
                             'Stoerung2' : ('Stoerung'),
                             'Strata1': ('Basis_so'),
                             'Strata2': ('Basis_smS'),
                             'Strata3': ('Basis_smD')
                         },
                         remove_unused_series=True)
# assign basement and faults

geo_model.add_surfaces('Basement')
geo_model.set_is_fault(['Stoerung1'])
geo_model.set_is_fault(['Stoerung2'])

# In[12]:


# plot interface points
gp.plot_2d(geo_model, direction='z', show_lith=False, show_boundaries=False, legend=True)
plt.grid()


# In[13]:


#plot interface points in 3D

gp.plot_3d(geo_model, image=False, plotter_type='basic', notebook=True)

# In[14]:


# interpolation

gp.set_interpolator(geo_model,
                    compile_theano=True,
                    theano_optimizer='fast_compile',
                    verbose=[],
                    update_kriging=False
                    )

# In[15]:


# computing the model

sol = gp.compute_model(geo_model, compute_mesh=True)

gp.plot_2d(geo_model, direction=['x', 'x', 'y', 'y'], cell_number=[25, 75, 25, 75], show_topography=
    False, show_data=False)
# In[16]:


# plot in 3d
```

```
gpv = gp.plot_3d(geo_model, image=False, show_topography=True,
                 plotter_type='basic', notebook=False, show_lith=True, show_data=False,ve=3)
```